Article

Optimization of Distributed Energy Resources in Distribution Networks Using Multi-Objective Archimedes Optimization Algorithm

Muhammad Shakeel[1,2] , **Ali Arshad[1]**, **Nida Tasneem[3]** and **Yazan M. Alsmadi[4]**

[1] Department of Electrical Engineering, COMSATS University Islamabad, Islamabad 45550, Pakistan;
[2] National University of Medical Sciences, Islamabad, Pakistan, muhammad.shakeel@numspak.edu.pk
[3] Department of Software Engineering, Foundation University, Islamabad, Pakistan; nida.tasneem@fui.edu.pk
[4] Department of Engineering, Computing and Mathematical Sciences (ECaMS), Lewis University, Romeoville, IL 60446, USA; yalsmadi@lewisu.edu
* Correspondence: yalsmadi@lewisu.edu

Abstract

DERs can improve the performance of radial distribution systems. The nonlinear power flow constraints, multi-objective trade-offs, and network reconfiguration scenarios for DER placement and sizing cause optimization problems. Most of the times Optimization Algorithms suffer from premature convergence and poor exploration-exploitation balance. These problems exibit an inherent internal structural symmetry. In order to overcome the above problem, this study uses the Multi-Objective Archimedes Optimization Algorithm (MAOA) to optimally allocate DERs in the RDN (Radial Distribution Networks), and the performance of the proposed MAOA is compared with the other well established algorithms including PSO, WOA, SFLA, ASO and BOA on the IEEE-33 RDN. The comparison is made for the four cases (S1:DER Only), (S2 – Network Reconfiguration Only) (S3 - DER Followed by Reconfiguration) (S4 - Reconfiguration Followed by DER) considering factors like Voltage Profile,Network reconfiguration,Active and Reactive Loss Reduction, carbon emission DER utilization and Cost reduction. The MAOA is observed to provide better results among all the other benchmark algorithms in scenario S3 (DER Followed by Reconfiguration). The active power loss is reduced by 68.41% from 208.459 KW to 65.482 KW, whereas the reactive power loss is reduced by 57.44% and the MAOA algorithm greatly optimizes the average voltage profile by 3.98% from 0.0497 pu to 0.9871 pu. The minimum voltage of the network is also improved by 6.28% from 0.9108 p.u. to 0.9680 p.u. The algorithm improves convergence with a percentage of 18.50% enhancing the system's operational symmetry and stability also satisfying all constraints. At Bus 3 and Bus 6 of IEEE-33 bus radial distribution network (Baran–Wu test system), DG capacity is allocated to be 3.8 MW and 2.1 MW, respectively.

Keywords: Distributed Energy Resources; Optimization Algorithms; Power Loss Reduction; Voltage Profile Improvement; Archimedes Optimization Algorithm

1. Introduction

Recent increases in distribution-level demand, urban electrification, and renewable integration have intensified operational stresses on radial distribution networks, particularly in terms of voltage deviations, losses, and reliability constraints. These challenges highlight the need for optimization-driven planning approaches that can determine the optimal

placement and sizing of Distributed Energy Resources (DERs). Distributed generation is the generation of electricity, as from a photovoltaic solar panel, a wind turbine, or a small scale hydroelectric scheme, close to or at the point of consumption rather than in a large central power station. This can reduce transmission and distribution losses, stabilize the grid and allow greater local control of supply. However, existing optimization methods still struggle with high solution dimensionality, non-convexity, and simultaneous coordination of placement and reconfiguration decisions.

The United Nations Framework Convention on Climate Change (UNFCCC) and the Intergovernmental Panel on Climate Change (IPCC) have promoted global initiatives aimed at carbon neutrality, energy transition, efficiency enhancement, and large-scale decarbonization. In recent years, global energy demand has risen to approximately 592 EJ, with an annual growth rate of about 2%, closely aligned with the increase in carbon emissions, which reached approximately 2.46% in 2024. The growing demand for cooling to cope with increasingly intense summer heat has further accelerated the consumption of fossil fuels, including oil, coal, and natural gas.

Distributed energy resources (DERs) represent a diverse group of small-scale, decentralized energy technologies that generate, store, and manage power at or near the point of consumption to reduce active and reactive power losses. DERs offer several advantages over traditional centralized power plants and transmission and distribution systems, including improved reliability, reduced transmission losses, and enhanced grid resilience and their symmetry. By 2024, the total installed capacity of renewables in Pakistan has increased, with a particular rise of solar projects, attaining an installed capacity of 1000 MW. The Government of Pakistan has announced an exemption of import duties for plant and equipment for the production of energy from renewable sources. The Green Energy Policy, 2021 has been announced to offer investments and financial incentives to provincial governments, institutions and end-users.

Radial systems are the simplest, primary distribution substations and are supplied from generating stations via inter-connected transmission systems. The substations supply customers with power via passive RDS, and the power flow is unidirectional. In a distribution network, the R/X ratio is high, and voltage excursions are larger than in transmission. Thus, in a distribution network a small perturbation in the loads may cause abrupt voltage collapse at many nodes. These nodes are less voltage stable nodes.

Distributed reactive power support (i.e. capacitors and switched capacitor banks) have also customarily been used to regulate voltage and reduce losses in the distribution systems. However, they have a limited ability to control the voltage (to 1.0 p.u.) and as RDS is passive the authors feel this is not good from a system performance and reliability viewpoint. As an alternative, RDS have been proposed with a view to system stability and voltage profile enhancement from renewable energy source based electric sources. The embedded RDS generation described above is referred to as distributed generation (DG).

Historically, various techniques have employed scattered resources and reactive power injection, such as capacitor banks, to improve voltages and reduce power losses. While capacitor placement offers reliability benefits, voltage profile improvements often fall short of desired levels (i.e., 1.0 p.u.). The inherent passivity of RDS limits its reliability. Recent solutions incorporate renewable energy-based electric sources to overcome RDS passivity and improve system functionality and voltage profiles. This embedded RDS generation is referred to as distributed generation (DG). This approach can reduce transmission and distribution losses, increase grid stability, and enhance local energy supply control.

In distribution systems, the R/X ratio is relatively higher than in transmission systems, resulting in greater power losses in distribution networks. Research indicates that 13% of total generated power is lost as I^2R losses in distribution networks [10]. These losses

directly impact energy costs due to voltage profile imbalances along distribution feeders. [81]
Reduction of the distribution losses has become a primary concern for ensuring efficient [82]
and cost-effective network operation [10]. Meanwhile, rapid load increases can exacerbate [83]
voltage instability. While various methods exist to reduce losses at higher voltage levels, [84]
including capacitor installation and reconductoring, network reconfiguration is commonly [85]
employed due to its cost-effectiveness and minimal equipment requirements [11]. The [86]
main objective of distribution system reconfiguration (DSR) involves optimizing radial op- [87]
erating frameworks to curtail overall power loss while maintaining operational constraints. [88]
Network reconfiguration combined with distributed generation installation represents the [89]
most effective approach for overcoming energy losses,enhancing symmetry of the network, [90]
improving undesirable voltage magnitudes, and enhancing overall distribution network [91]
efficiency [12]. Optimizing network configuration, DG unit sizes, and locations is crucial [92]
for maximizing benefits while minimizing system impacts, making this combination an [93]
important and complex problem. [94]

Network reconfiguration involves adjusting the open/closed positions of sectional- [95]
izing and tie-line switches in distribution networks to alter system configurations. This [96]
method can improve network efficiency by addressing various specific objectives and con- [97]
straints. Primary reconfiguration objectives typically include improving voltage magnitude [98]
levels, reducing power losses, balancing loads, and enhancing voltage stability [13]. Over [99]
the past two decades, researchers have employed numerous techniques to solve network [100]
reconfiguration problems, including load balancing methodologies [14–16]. [101]

Installing distributed generation (DG) units represents another effective technique [102]
for improving network voltage profiles and reducing power losses. DG units comprise [103]
small power generation systems connected directly to distribution networks or customer [104]
meter locations. DG application in distribution networks is growing rapidly, with ongoing [105]
studies examining their environmental, practical, and economic effects on energy systems. [106]
Optimal DG unit location, type, and size significantly impact electrical energy networks' [107]
economic and technical performance. Recent research has extensively investigated DG [108]
component effects. [109]

[17] proposed a logical and enhanced analytical approach for determining DG unit [110]
sizes and locations to limit network power losses. [18] presented a Particle Swarm Opti- [111]
mization (PSO) approach to identify optimal locations for different DG types to address [112]
power loss problems. [19] employed a new modified teaching–learning-based optimiza- [113]
tion technique to determine optimal DG locations and sizes. [20] introduced a hybrid [114]
population-based approach integrating Particle Swarm Optimization and gravitational [115]
search algorithms to optimize DG sizes and placements in distribution networks. More [116]
recently, [21] examined DG installation issues across different load percentages using a [117]
Bacterial Foraging Optimization Algorithm (BFOA) approach. [118]

Previous studies have primarily focused on DG installation without considering [119]
network reconfiguration for optimal new DG location identification. However, achieving [120]
maximum efficiency from entire distribution frameworks requires incorporating both DG [121]
installation and network reconfiguration considerations [22,23]. [24] utilized Harmony [122]
Search Algorithm (HSA) to simultaneously identify optimal DG locations and network [123]
reconfigurations, considering power loss minimization as the sole objective function. [25] [124]
employed an energy storage model based on demand response management systems using [125]
cost and distributed solar systems to provide uninterrupted power supply to communities. [126]

[26] addressed optimization challenges in distribution network configurations using [127]
the self-adaptive Kho-Kho optimizer, aiming to minimize operational costs while improving [128]
multiple parameters including voltage stability and loss reduction. Their proposed method [129]
demonstrated significant improvements through 226 kVAR capacitor placement and 110 kW [130]

distributed generation unit installation at Bus 14, achieving 25.54% power loss reduction. Their research applied multi-objective algorithms and distributed generations to the IEEE-33 bus standard network to improve reliability and stability [26].

Addressing inefficiencies and instabilities arising from inductive loads such as transformers and motors, [27] investigated parallel capacitor integration for optimal capacitor placement within distribution networks to minimize losses and improve voltage stability. Using DIgSILENT PowerFactory and MATLAB optimization algorithms for capacitor location and sizing in 33-bus distribution networks, their study found that incorrect placement and sizing can increase voltage deviations with higher harmonic levels. Without considering harmonic loads, optimization reduced network losses by 33%. Their research demonstrated that targeting capacitors alone cannot improve efficiency, requiring combined indexed objective functions accounting for both losses and voltage deviations. Optimal placement of two capacitors achieved 37% loss reduction relative to harmonic baselines while maintaining voltages above 0.95 p.u. and total harmonic distortion below 5% [27].

[28] presented a heuristic search method for distributed energy resource sizing, identifying multiple microgrid design options through power load set definitions. They developed a global binary search algorithm for multiple microgrid design options, refined through local linear search methods. For military installation planning needs, they explored sizing methods constructing customizable search heuristics adaptable to additional technologies. These heuristics, planned according to current microgrid investments, efficiently handle DER technology portfolio sizing, with their method realized in the Microgrid Planner [28].

[29]selected the Gray Wolf Optimizer for its global search capability, comparing simulations on IEEE-33 and IEEE-69 bus systems against Cuckoo Search Algorithm, Multi-Objective Particle Swarm Optimization (MOPSO), and Genetic Algorithm (GA). Results showed the Gray Wolf Optimizer achieved minimal power loss (85.4 and 78.3 kW) and highest renewable energy source absorption rates (88% and 89%) while maintaining voltage quality and optimizing investment costs. Their study demonstrated GWO's superior efficiency among optimization algorithms, showing highest efficiency-stability ratios for distribution networks and reduced fossil fuel dependency.

Hybrid renewable energy systems face challenges in load management, energy management, efficiency, and reliability. [30] focused on solutions using Ant Lion Colony Optimization with Particle Swarm Optimization for maximum power point tracking to improve power efficiency, despite computational complexity and premature convergence costs. Their study also detected current faults using artificial neural networks with solar data, achieving 99.5% accuracy and faster convergence (0.11 s) [30].

[31] focused on reducing power loss, energy loss, and total electricity purchase costs using the War Strategy Algorithm (WSO). WSO identified smaller losses and reduced one-day energy loss and grid energy purchase costs for IEEE-69 node distribution generation planning. Their study also optimized soft open point locations, optimizing location and capacity of renewable energy-based distributed generators in IEEE-33 and IEEE-69 node distribution power grids. Results showed 96.1% energy loss reduction, with cost reductions of approximately 61.44% and 9.2% of total grid costs. Optimal connection and capacity determination of renewable energy-based distributed generators significantly reduced energy loss and energy purchase costs from conventional power grids [31].

[32] applied the Dandelion Optimizer for optimal energy storage system placement and sizing in distribution networks, reducing expenses including power losses, voltage deviation, and peak load demand. Their analysis on the IEEE-33 bus distribution system demonstrated that this technique outperformed alternatives such as the Ant Lion Optimizer,

showing that efficient sizing and optimized placement of energy storage systems can enhance distribution system performance [32].

[33] addressed voltage uncertainty and power loss issues through effective network reconfiguration integrated with distributed generation. Their study emphasized proper installation with appropriate locations and capacities, utilizing the Artificial Hummingbird Algorithm implemented via DG-1 and DG-2 in radial distribution networks. Their proposed AHA and WaOA approaches provided efficient and optimal DG allocation tested on the IEEE-69 bus network [33].

[34] investigated four heuristic-based algorithms—Particle Swarm Optimization (PSO), Whale Optimization Algorithm (WOA), Dolphin Echolocation Optimization (DEO), and Slime Mould Algorithm (SMA)—for optimal DG unit placement and sizing. Testing algorithm feasibility on IEEE-69 and IEEE-33 bus test systems showed their proposed SMA outperformed other algorithms, achieving 81.1% real power loss reduction and voltage profile improvement to 0.977 p.u. in IEEE-33, and 97.30% power loss reduction with minimum voltage profile improvement to 0.995 p.u. in IEEE-69 [34]. The extensions studied include EV scheduling RES and grid integration, 24-hour load coordination, but those have been relegated to follow-up research, since the focus in this paper is on steady-state DER placement and network reconfiguration. Combining DG and demand-side management (DSM) can further optimize grid usage by enabling more efficient local resource utilization and reducing expensive transmission and distribution infrastructure requirements. Additionally, this combination can improve energy system resilience and security. [35] optimized multi-objective evolutionary algorithms for DG placement considering reconfiguration of IEEE-33 and IEEE-118 bus radial systems, improving load site voltages while increasing losses. [36] incorporated Gaussian mutation strategies with Particle Swarm Optimization to improve PSO performance, implementing their improved technique on IEEE-33 bus networks to reduce losses and improve system stability across various loads. Their hybrid model and modified PSO parameter weights increased convergence time compared to basic PSO implementations [36]. [?] implemented the Slime Mould Algorithm (SMA) on IEEE-33 and IEEE-69 bus networks for DER placement, including wind and solar energy, testing under dynamic load conditions. Generating dynamic loads for standard RDS reduced optimization algorithm efficiency due to load fluctuations between upper and lower limits [?].

Table 1. Comparative Analysis of Literature on DER Placement Optimization

Reference Paper	IEEE Model	Static Load	Active Losses	Voltage	Cost	Emissions	DER	Reconfig.	Algorithm
[10]	✓	✓	✓					✓	OPF
[38]				✓			✓	✓	Markov
[39]	✓		✓	✓			✓	✓	PSO
[40]	✓	✓	✓	✓	✓		✓	✓	PSO
[41]	✓	✓	✓	✓			✓		GA
[42]	✓	✓	✓	✓			✓		GA
[43]	✓	✓	✓						OPF
[44]	✓	✓	✓	✓			✓		HSA
[45]	✓		✓	✓			✓		SSA
[46]	✓		✓	✓	✓		✓		AIMD
[47]		✓	✓		✓				OPF
[48]	✓	✓	✓		✓		✓		ABC
[49]	✓		✓	✓			✓		ANN
[50]	✓								DSO
[51]		✓	✓	✓			✓		IPSO
[52]			✓	✓					Root
[35]	✓	✓	✓	✓	✓		✓		MOEA
[36]	✓		✓	✓	✓		✓		IPSO
[?]	✓		✓	✓	✓			✓	SMA
Proposed Work	✓	✓	✓	✓	✓	✓	✓	✓	**AOA**

Table 1 summarizes key optimization approaches reported in the DER placement and distribution system optimization literature. While the list is representative of mainstream

metaheuristic families—including swarm-based, evolutionary, physics-inspired, and hybrid techniques. Many algorithmic variants exist, and the table focuses on those most frequently applied to DER planning problems in peer-reviewed studies. While comparing the algorithms, it has been noticed that optimization algorithms can be differentiated on the bases of there behaviors, like (i) the intrinsic mathematical properties of the update equations of each algorithm, (ii) Exploration-exploitation behaviors are thus well-documented in the optimization literature, and (iii) underlies the patterns of convergence documented here. These describe relative tendencies rather than numerical indices. Such a comparison, at the level of the mechanism, is clearly favorable to MAOA. In PSO, WOA, BOA, and SFLA, the search behavior is largely controlled by static coefficients, or control policies that correspond to static stochastic operators, is limited. The multi modal and mixed-variable nature of the DER placement problems is also been addressed. On the other hand, the MAOA search pressure in real time as measured by improvement in fitness, allowing it to balance exploration and exploitation systematically.

Additionally, the feasibility-coupled update rule in MAOA allows for high movement in valid operational boundaries of the distribution network, reducing the number of infeasible solutions and accelerating convergence. These mechanisms collectively explain why MAOA appears lower operational losses, improved voltage stability and a more reliable convergence in the IEEE-33 case study.

This follow-up analysis further shows MAOA's suitability for more complex network configurations. configurations, which may be unbalanced, large-scale, or meshed. The subset was selected based on citation frequency, demonstrated performance, and relevance to mixed discrete–continuous problems. Although the proposed MAOA shows strong performance compared to these well-established methods, the broader research landscape indicates that further exploration of hybrid, adaptive, and problem-tailored algorithms remains an open direction.

This study provides a novel approach for optimal DER placement and sizing in radial distribution networks, incorporating the following considerations:

- Radial network configuration remains essential, with network connectivity managed through tie switches by algorithms.
- Optimal placement determination incorporates loss sensitivity factors, voltage sensitivity indexes, and maximum loss busses.
- Optimal DER sizing is determined by total system load versus DER upper and lower limits.
- The methodology contributes to carbon emission reduction aligned with global Sustainable Development Goals (SDGs), aiming to reduce carbon footprints.
- Cost considerations for both users and utilities/governments are incorporated into fitness function implementation, including loss considerations.

This study encompasses technical analysis while considering environmental impacts, maintaining system stability according to IEEE standards. The methodologies introduced hold significant potential for driving progress towards reliable power systems while aligning with global sustainability initiatives.

2. Problem Formulation

2.1. Problem Statement

The integration of DERs in the distribution grid has the potential to provide cost effective reliable power supply. However, the placement of DERs in the distribution network is a complex problem that involves technical factors such as choice of DER, optimal sizing, siting and network reconfiguration issues. Power flow improves after

installing DERs in the distribution network but optimal locations and size of DER are still an open research problem. We propose the use of Archimedes Optimization Algorithm (AOA) based on factors like active and reactive power losses, voltage profile, costs and network reconfiguration to find the optimal locations and size of DERs. Optimal DERs placement is a sustainable solution complying to Sustainable Development Goad (SDG)-7 (energy), SDG-13 (climate change) and earlierMillennium Development Goal (MDG)-7 (environment). A base model without DG is compared with AOA optimised results to determine the reduction in losses and increase in efficiency. Pakistan consumes 127 TWh electric energy which increases to 149 TWh at powerhouse levels and 192 TWh at primary energy consumption level as 66% energy is lost between primary energy source and meter. Global electricity demand is 30,761 TWh in 2025, which at an average 10%-line losses has the potential to save 154 TWh using DERs out of total 3,076 TWh losses. The proposed methodology not only provides an optimal solution for integrating renewable energy sources in the distribution network, while ensuring a stable and reliable power grid, but also 50–60% reduction in electricity losses which results in lesser fossil fuel demand.

Beyond operational cost reduction, strategically placed DERs can also defer or avoid capital expenditures associated with upgrading transmission or distribution infrastructure. Although this study focuses on operational metrics, such long-term investment benefits are an important complementary aspect of DER planning.

2.2. Power Flow Fundamentals

Let us consider there are two buses m and n with a distribution line having resistance R_{mn} and reactance X_{mn}. The voltage at bus m and n is given by V_m and V_n respectively, Current flowing from the branch is I_{mn}. Load at Bus n is connected having active load P_L and reactive load Q_L. the power flowing from branch will be P_{mn} and Q_{mn} respectively, as shown in Figure 1. Whereas P_{mn} is the total active while Q_{mn} is the total reactive power flow through the branch active and reactive power loss in branch can be calculated as under:

Apparent power flow can be given as

$$S_{mn} = P_{mn} + jQ_{mn} \tag{1}$$

The magnitude of the apparent power will be:
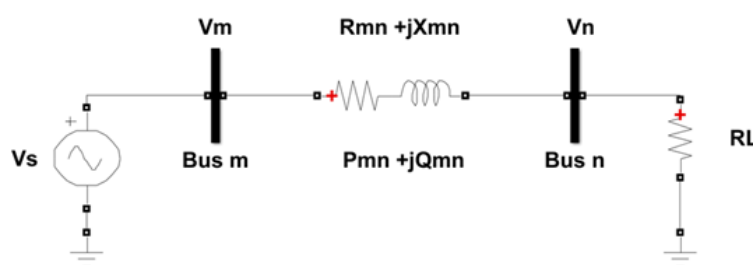
$$|S_{mn}| = \sqrt{P_{mn}^2 + Q_{mn}^2} \tag{2}$$

Figure 1. Two Bus Model Power Flow (Hadi Saadat, 1999) [60]

Active power loss can be calculated with apparent power as below

$$PLoss_{mn} = R_{mn} \left(\frac{|S_{mn}|^2}{V_m^2} \right) \tag{3}$$

By putting values, we get:

$$PLoss_{mn} = R_{mn}\frac{P_{mn}^2 + Q_{mn}^2}{V_m^2} \tag{4}$$

Similarly, reactive loss between bus m and n will be:

$$QLoss_{mn} = X_{mn}\frac{P_{mn}^2 + Q_{mn}^2}{V_m^2} \tag{5}$$

Reactive Power has many disadvantages in Power System. As reactive power moves in between two buses of power network from one end to other end, this extra current increases the copper losses I^2R that results in poor efficiency. Secondly the poor voltage regulation and handling capacity of system. It also affects the KVA rating of equipment and needs large conductor size.

So, total active and reactive power flow between two nodes will be sum of active load and reactive load and loss in the branch.

$$P_{mn} = P_{Load} + PLoss_{mn} \tag{6}$$

$$Q_{mn} = Q_{Load} + QLoss_{mn} \tag{7}$$

After substituting values, we have

$$P_{mn} = P_L + R_{mn}\frac{P_{mn}^2 + Q_{mn}^2}{V_m^2} \tag{8}$$

$$Q_{mn} = Q_L + X_{mn}\frac{P_{mn}^2 + Q_{mn}^2}{V_m^2} \tag{9}$$

If network has i number of buses, then the power loss of the network can be calculated as sum of losses between all nodes and all branches, total active and reactive power loss the system will be called as,

$$TotalP_{loss} = \sum_{i=1}^{No\ of\ branches} P_{loss,i} \tag{10}$$

$$TotalQ_{loss} = \sum_{i=1}^{No\ of\ branches} Q_{loss,i} \tag{11}$$

P_{mn}, Q_{mn}, and S_{mn} are the active, reactive and apparent power that flow between buses m and n. I_{mn} is the line current. P_L and Q_L are the active and reactive load demand at the bus. Q_{Loss}, $Q_{\text{Loss,Base}}$, and $Q_{\text{Loss,min}}$ are the total, base-case, and minimum reactive power losses of the distribution system.

Distributed Generation Placement

Here, the main requirement is to detect the optimal location for DG placement in the distribution network. In the proposed approach, the DG is placed at the branch exhibiting the maximum active power loss, which is referred to as the Loss Sensitivity Factor (LSF). The LSF-based selection ensures that DG units are installed at electrically weak locations where loss reduction potential is maximum. Accordingly, the candidate bus for DG installation is identified as

$$DG_{\text{Candidate Bus}} = \text{Bus with } \max(P_{\text{loss}}). \tag{12}$$

Once the candidate location is determined, the DG size is selected such that it remains within the loss contribution of the corresponding branch, thereby avoiding excessive power injection and adverse operating conditions. This sizing constraint is expressed as

$$DG_{\text{size}} \ (\text{kW}) \leq P_{\text{loss}} \ \text{of the branch.} \tag{13}$$

Based on this formulation, dispatchable DERs are modeled as controllable active power sources with bounded operating limits suitable for planning-level optimization. The objective is to determine optimal DG placement and sizing under steady-state operating conditions using power-flow analysis. Detailed temporal dispatch characteristics and unit commitment constraints are not considered in this study, as the focus is on planning-oriented optimization rather than real-time operational control.

Reconfiguration of Tie Switches

Power system reconfiguration is another key aspect in the distribution system to provide uninterrupted power with minimum losses and maximum voltage. This change of load flow direction depends on the number of tie switches of the distribution network. Here, the main requirement is to detect the optimal configuration of the network using power flow analysis by considering different combinations of tie switches, the optimal combination detected having minimum overall network loss.

Radial distribution networks contain two types of switching elements: sectionalizing switches (normally closed), forming the radial backbone, and tie-switches (normally open), used to interconnect non-adjacent feeders when closed. Let the complete set of switches be

$$\mathcal{S} = \{S_{ij} \mid (i,j) \text{ is a branch or tie-line}\},$$

where each switch has a binary state, closed (energized) or open. Closing or opening switches modifies the radial structure, thereby changing the power flows, voltage drops, and corresponding losses computed using the loss model (4.7a)–(4.7b).

The set of active energized lines is

$$\mathcal{L}_{\text{active}} = \{(m,n) \mid S_{mn} = 1\}.$$

The real total losses for any switching configuration become

$$P_{\text{loss,tot}}(S) = \sum_{(m,n) \in \mathcal{L}_{\text{active}}} P_{\text{loss},mn}.$$

Accordingly, the reconfiguration objective is expressed as

$$Configuration_{Tie-switches} = Network \ with \ Minimum(P_{loss}) \tag{14}$$

Where,

$$P_{loss\_new\_configuration} \ (KW) \leq P_{loss\_base\_configuration} \tag{15}$$

When a normally open tie-switch is closed, a loop is created because the base radial network originally satisfies

$$|\mathcal{L}_{\text{active}}| = N_b - 1.$$

Closing a tie-switch yields

$$|\mathcal{L}'_{\text{active}}| = N_b,$$

which must contain exactly one loop. Every branch in the loop is a candidate for opening to restore radiality. Thus every tie-switch closing generates a loop, and exactly one sectionalizing switch is opened to maintain radiality.

To retain a radial structure:

$$\sum_{(i,j)} S_{ij} = N_b - 1 \tag{16}$$

Every bus must remain connected to the slack bus. These constraints ensure a single spanning tree covers all buses.

For the IEEE 33-bus distribution network, the reconfiguration process is implemented using a switch topology below mentioned matrix that maps switch positions to branch numbers:

$$\text{Tie-Switches} = \begin{bmatrix} 8 & 9 & 10 & 11 & 21 & 33 & 35 & 0 & 0 \\ 2 & 3 & 4 & 5 & 6 & 7 & 18 & 19 & 20 \\ 12 & 13 & 14 & 34 & 0 & 0 & 0 & 0 & 0 \\ 15 & 16 & 17 & 29 & 30 & 31 & 36 & 32 & 0 \\ 22 & 23 & 24 & 25 & 26 & 27 & 28 & 37 & 0 \end{bmatrix}$$

Generation Cost

To minimize the operational cost of power production [49] at any bus i per hour can be given as:

$$G_{Cost,i} = (a_i + b_i Pg_i + c_i Pg_i^2) \text{ USD/Hour} \tag{17}$$

Where a_i, b_i and c_i are the cost function coefficients of the generator at bus i. $GCost_i$ represents the hourly generation cost associated with the generator installed at bus i. Similarly, for n_g number of generators, the overall cost function will be the sum of all the cost per generator to get the total cost of production per hour, given as:

$$Total\ Cost = \sum_{g=1}^{n_g} F_{cost,g} \text{ USD/Hour} \tag{18}$$

$F_{\text{cost},g}$ denotes the cost-related objective component associated with generator g in the overall multi-objective fitness function. In addition to operational cost reductions, the integration of DERs may also contribute to capital cost savings by deferring or avoiding investments in transmission and distribution infrastructure expansion; however, a detailed analysis of such capital expenditure benefits is beyond the scope of this study.

Emission Function for Generation

To minimize the operational emission during power production by any thermal generator at any bus g per hour [53] can be given as:

$$F_{Emission,g} = a_g + b_g Pg_g + c_g Pg_g^2 + d_g \exp(e_g Pg_g) \tag{19}$$

Whereas a_g, b_g, c_g, d_g and e_g are the emission function coefficients of the generator at bus g. Similarly, for n_g number of generators, the overall emission function will be sum of all the emission/ generator to get total emission production per hour as:

$$Total\ Emissions = \sum_{g=1}^{n_g} F_{Emission,g} \text{ Ton/Hour} \tag{20}$$

Solar Power

Power generated by solar panel depends on the irradiance, temperature, and efficiency of the solar panel. Let a solar power is installed at Bus i, have a total area A of the panels in square meters with solar panel yield r, where average annual solar radiations is H kWh/m2, and Performance Ratio, a coefficient for losses PR, The electric energy provided by that solar plant will be calculated as:

$$P_{solar,i} = A \cdot r \cdot H \cdot PR \tag{21}$$

The Weibull distribution, often used for wind statistics, has been used in solar energy as a statistical model for irradiance H to add an uncertainty factor.

Wind Power

Wind power depends on the airflow in swept area A, air density ρ [kg/m3], wind speed v [m/s] and the time t. Here the circular area of the wind turbine is based on radius r of the wings/blade of turbine,

$$A = \pi r^2 \tag{22}$$

Therefore, the electric energy produced by wind power plant will be calculated as

$$P_{wind,i} = \frac{1}{2} A \rho v^3 t \tag{23}$$

The Weibull distribution will be used in wind energy as a statistical model for wind speed to add uncertainty factor in wind speed for simulation.

2.3. Importance of Local Reactive Power Management

Radial feeders' voltage stability at feeder ends is much more sensitive to reactive power compensation. When DERs are run in Q-control mode, they could consume (or produce) local reactive power to greatly reduce upstream reactive current on branches. This reduces the voltage drop of the line and the voltage stability margins. The fitness function was modified to penalize undervoltages at the feeder end and to account for the Q-injection limits of the DERs in the power flow equations. Including this gives a better idea of the local voltage support capabilities.

The Fitness Function

Objective function of the power system for DER will be to minimize the network losses and improve minimum voltage of the system. Where, N_{br} is total number of branches in network. This is multi objective function problem given as,

$$F(\text{Fitness}) = \text{Total } P_{loss} + \text{Total } Q_{loss} \\ + \text{Total Cost} + \text{Total Emissions} \tag{24}$$

Fitness function is a unitless quantity used to derive and optimize algorithm. Every contributing factor has same weightage of 25% as contributing factor towards Fitness Function.

By putting values from equations (11), (12), (17) and (19), we have fitness function as under:

$$F(\text{Fitness}) = F_a \sum_{i=1}^{N_{br}} P_{loss,i} + F_b \sum_{i=1}^{N_{br}} Q_{loss,i} \\ + F_c \sum_{i=1}^{N_{bus}} G_{cost,i} + F_d \sum_{i=1}^{N_{bus}} F_{emission,i} \tag{25}$$

Here, Fa, Fb, Fc, and Fd represented the weighted contributing factor as 25% = 0.25 each. Here, N_{br} is total number of branches and N_{bus} are total buses of network. In fitness function use normalize sub objectives through average of cost functions.

Constraints of Fitness Function

Bus voltage will remain in between minimum and maximum values as given in below equation.

$$V_{minimum} \leq V_{bus} \leq V_{maximum} \tag{26}$$

Power generation by DERs should remain within upper and lower bounds i.e.

$$Pg_{minimum} \leq Pg \leq Pg_{maximum} \tag{27}$$

Active Loss should be less than Base loss of the model i.e.

$$PLoss_{minimum} \leq PLoss_{Base} \tag{28}$$

Reactive loss should be less than Base loss of the model

$$QLoss_{minimum} \leq QLoss_{Base} \tag{29}$$

Variable load of the network should be in between the upper and lower bound of the network,

$$Pload_{minimum} \leq Pload_{i,Bus} \leq PLoad_{maximum} \tag{30}$$

All numerical results have been rounded to reflect realistic engineering precision rather than raw computational precision. This ensures that reported values represent physically meaningful accuracy.

3. Research Methodology

Optimal placement of DERs in distribution system is initiated by identifying the weaker or sensitive buses to minimize real and reactive power losses, improve voltage profile throughout the network and enhance system stability. Optimal placement and DER sizing study is initiated with sensitivity- based analysis to detect the weakest bus then using optimization algorithms to determine the size and location of DER. Active and reactive line losses are minimized with local power to reduce flow of power from remote powerhouse in far flung areas to load in populated cities. Voltage in weak weaker systems dips with load variations which increases line losses. Suitably designed DER enhances system resilience to varying loads and line faults. Power engineers use the continuation power flow (CPF) method to conduct sensitivity analysis. Analytical methods using commercial software are used to conduct load flow study without and with DERs to estimate reduction in power losses and improvement in voltage profile. We may limit constraints in multi-objective function for optimal voltage, line losses, system stiffness and other stability parameters. Algorithms keep on iterating until the objectives are achieved. We have Modified AOA in MATLAB to optimize the DER placement.

The Archimedes Optimization Algorithm (AOA) is a physics-inspired metaheuristic based on Archimedes' principle [59]. According to Figure 2, the algorithm simulates objects immersed in fluid, where buoyancy forces drive the optimization process.
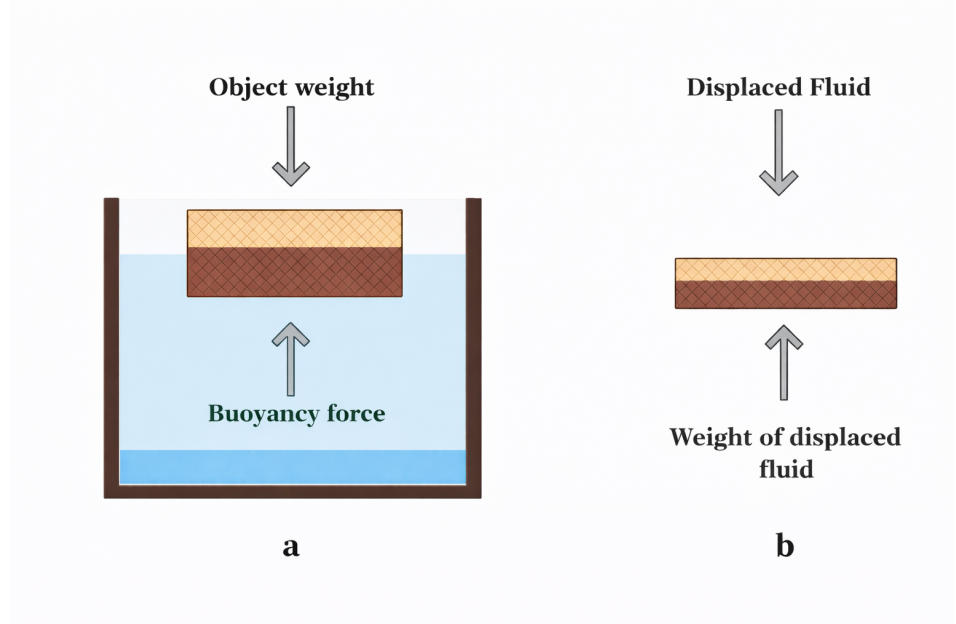
Figure 2. (a) An object immersed in a fluid, and (b) The volume of fluid displaced [59]. Note: The figure illustrates the physical principle of buoyancy used as inspiration for the algorithm's density and volume updates.

The working principle or concept behind the algorithm is based on Archimedes' Principle. In AOA, a candidate solution is represented as an object submerged underwater; the object "density" and "buoyancy" guide the object towards better solutions. Mathematically, the density, volume, and buoyant force, reflect how the algorithm calculates the new position of an object based on density and the amount of buoyant force.

The Archimedes Optimization Algorithm (AOA) is inspired by Archimedes' principle; however, in this study, its governing operators are explicitly mapped to power system performance indicators rather than treated as abstract physical metaphors. Each candidate solution is represented by a decision vector

$$\mathbf{x} = \left[\text{bus}_i,\ P_i^{DG}\right], \tag{31}$$

which defines the locations and sizes of distributed energy resources (DERs) in the distribution network. The quality of each candidate solution is evaluated through load-flow analysis, and its overall performance is quantified using a fitness function $F(\mathbf{x})$ that incorporates active power losses, voltage deviations, and operational constraints.

In this formulation, the *density* parameter $\rho(\mathbf{x})$ reflects the electrical quality of a solution and is expressed as a function of system losses and constraint violations, i.e.,

$$\rho(\mathbf{x}) \propto P_{\text{loss}}(\mathbf{x}) + \lambda_v \sum_i \Delta V_i + \lambda_l \sum_l \Delta I_l, \tag{32}$$

where P_{loss} denotes the total active power loss, ΔV_i represents voltage magnitude violations, ΔI_l corresponds to branch thermal limit violations, and λ_v and λ_l are penalty coefficients. Solutions exhibiting lower losses and minimal violations are associated with lower effective density and are therefore favored during the optimization process. The *volume* parameter $V(\mathbf{x})$ represents the feasibility margin of a solution, remaining stable for configurations that satisfy voltage, thermal, and radiality constraints, while being adaptively penalized for infeasible operating states.

3.1. Limitations of Standard AOA for DER Placement

While AOA strikes a balance between exploration and exploitation, it doesn't perform up-to the standard on DER placement problems because of: (i) weak local search capability near feasibility boundaries, (ii) insufficient diversity preservation in high-dimensional radial networks, (iii) slower convergence when mixed discrete-continuous variables (i.e. bus indices and sizes of the DERs) are involved. (iv) sensitivity to density and volume parameters under multimodal objectives.

To address these limitations, the Multi-Objective AOA (MAOA) introduces:

- an adaptive search pressure coefficient to accelerate convergence when refining the feasible region,
- a boundary-aware perturbation operator for discrete bus selection,
- a dynamic density update rule that increases exploitation in potentially good configurations, and
- a hybrid feasibility correction step tightly coupled with the power-flow constraints.

These improvements further improve MAOA's ability to navigate the fitness landscape of DER placement and network reconfiguration, yielding both higher quality and more stable solutions.

Although this analogy of buoyancy is useful in understanding the concept, it is also possible to interpret the density update process from the perspective of the search for fitness landscape optimization. The search step sizes are proportional to the recent gradient of fitness improvement achieved, pushing the particles towards lower objective function values. Volume and acceleration operators guide search: the volume operator impacts sampling distribution early on while the acceleration operator ramps up exploitation as convergence occurs. These operators, although lacking a physical interpretation, are mathematically consistent and considerably improve search performance for constrained DER optimization.

3.2. Algorithm Fundamentals

According to Archimedes' principle, the buoyancy force equals the weight of displaced fluid:

$$F_b = \rho_f V_d g \tag{33}$$

For an object in equilibrium:

$$\rho_o V_o a_o = \rho_f V_f a_f \tag{34}$$

3.3. Mathematical Formulation

3.3.1. Initialization

N denotes the population size, while x_i^0 and x_i^t represent the initial and iteration-t positions of solution i. The term a_i^{norm} refers to the normalized acceleration, with u and l indicating normalization bounds, and F controlling the exploitation phase of the algorithm. For N objects (potential solutions), initial positions are generated:

$$x_i^0 = lb + \text{rand} \cdot (ub - lb), \quad i = 1, 2, \ldots, N \tag{35}$$

Initial parameters: Where ρ_i^0, V_i^0, a_i^0 are the density, volume, and acceleration of solution i at initialization, and rand $\in [0, 1]$ is a uniform random number, lb and ub are the lower and upper bounds of every dimension of the decision variables, respectively, ρ_i^t and V_i^t are the density and the volume of solution i at iteration t, respectively, and ρ_{best} and V_{best} are the density and the volume of the best solution. These functions are used to shift

the solution properties over time into promising parts of the search space to achieve a good balance between exploration and exploitation.

$$\rho_i^0 = \text{rand}, \quad V_i^0 = \text{rand}, \quad a_i^0 = lb + \text{rand} \cdot (ub - lb) \tag{36}$$

Density and volume updates:

$$\rho_i^{t+1} = \rho_i^t + \text{rand} \cdot (\rho_{\text{best}} - \rho_i^t) \tag{37}$$

$$V_i^{t+1} = V_i^t + \text{rand} \cdot (V_{\text{best}} - V_i^t) \tag{38}$$

3.3.2. Acceleration Update

Transfer factor determines search phase:

$$TF = \exp\left(\frac{t - t_{\max}}{t_{\max}}\right) \tag{39}$$

Exploration phase ($TF \le 0.5$):

$$a_i^{t+1} = \frac{\rho_{mr} + V_{mr} + a_{mr}}{\rho_i^{t+1} + V_i^{t+1}} \tag{40}$$

Exploitation phase ($TF > 0.5$):

$$a_i^{t+1} = \frac{\rho_{\text{best}} + V_{\text{best}} + a_{\text{best}}}{\rho_i^{t+1} + V_i^{t+1}} \tag{41}$$

3.3.3. Position Update

Normalized acceleration:

$$a_i^{\text{norm}} = u \cdot \frac{a_i - \min(a)}{\max(a) - \min(a)} + l \tag{42}$$

Position update (exploration):

$$x_i^{t+1} = x_i^t + C_1 \cdot \text{rand} \cdot a_i^{\text{norm}} \cdot d \cdot (x_{\text{rand}} - x_i^t) \tag{43}$$

Position update (exploitation):

$$x_i^{t+1} = x_i^t + F \cdot C_2 \cdot \text{rand} \cdot a_i^{\text{norm}} \cdot d \cdot (T \cdot x_{\text{best}} - x_i^t) \tag{44}$$

3.4. Multi-Objective AOA for DER Placement

The AOA is adapted for DER placement by mapping physical properties to electrical engineering components. Under this hypothetical optimization configurational space, the objects are DER configurations as defined by their siting and sizing. The density of the object represents a fitness of the solution, determined through the evaluation of the fitness function, while the volume is representative of the search space that will be explored. The acceleration term regulates the direction and magnitude by which the solution improves at each iteration. The surrounding fluid plays the role of the constraints that the distribution network must remain with in range of voltage with respect to load.

The others are implicitly defined through the fitness function, the scaling of the update size, and the constraints-edging methods. Each object denotes a candidate DER configuration. ρ_i: Solution quality relating to loss reduction, voltage profile improvement, and cost reduction. Similar to the definition of the electrical severity of loading in the

system network. V_i: Solution search adaptivity indicating the feasible operating margin of placing DERs under the network's operating restrictions. a_i: Solution search adaptivity indicating the direction and rate of convergence of the solution to the electrically optimal solution.

The transition between exploration and exploitation is controlled by a transfer factor TF, just as there is a mode between wide area network scanning and more local exploration around electrically stable operating points. During the exploration mode, acceleration is determined by random samples of point solutions, with heterogeneous feasible DER locations. On the contrary, the acceleration in the exploitation is controlled with respect to the best solution. It forces the swarm towards the minimum-loss, voltage-compliant solutions. The normalized acceleration a_i^{norm}, the control parameters C_1, C_2, F, and the direction factor d adjust the step size of the position update to remain within the voltage, power, and radiality limits of the distribution system. For all system parameters, standard IEEE radial distribution test feeders are adopted to ensure full reproducibility of the benchmark. For renewable generation, the parameters of photovoltaic generator efficiency, performance ratio, air density and Weibull distribution shape and scale coefficients are selected from the literature with a range of values. Algorithmic parameters, such as population size, number of iterations and search coefficients, are all dimensionless and are set empirically to ensure stability of convergence. These values are constant across all simulations.

The Initial population O_i^{PS} utilizes mixed power system variables, and calculates the system-aware density PS_den_i, volume PS_vol_i and acceleration PS_acc_i from the available power system operation variables. In both iterations, the transfer operator TF^{PS} and density factor d^{PS} control the exploration and exploitation based on the violation of the voltage and power balance. Finally, the updated solution values PS_den_i and PS_vol_i satisfy the feasibility and diversity conditions. We penalize infeasible motion with the constraint-aware acceleration, which uses the normalized term PS_acc^{norm} to update positions in mixed-variable domains: discrete indices (DG bus) are updated using the rounding operator, continuous DG sizes via real-valued arithmetic, and tie-switch states (binaries) by the sigmoid function. The candidate solutions are evaluated using the fitness function $F_{AOA}^{PS}(x)$ in conjunction with the dynamic weights $w_m(t)$, the normalization f_m^{base} and the adaptive penalties $\lambda(t)$. In cases where a candidate solution is found to be both fittest and feasible, this solution will replace the global best solution x_{best}^{PS} found so far. Periodic local search starts from this solution and perturbs with Gaussian noise $\mathcal{N}(0, \sigma^2)$, where σ is reduced for finer tuning. Iteration continues until convergence criteria based on improvement to the fitness function and satisfaction of constraints met for the power system, following which the best solution is returned.

Table 2. Multi-Objective Archimedes Optimization Algorithm for DER Placement

Algorithm : Multi-Objective Archimedes Optimization Algorithm for DER Placement
1. Initialize positions $\mathbf{x}_i^0$ using Equation (23)
2. Initialize ρ_i^0, V_i^0, a_i^0 using Equation (24)
3. Evaluate initial power flow via Equations (1)–(10)
4. Compute initial losses via Equations (11)–(12)
5. Apply DG and DER limits using Equations (14), (16), (21)
6. Enforce operational limits using Equations (23) and (25)
7. Evaluate initial multi-objective fitness via Equation (20) and set $\mathbf{x}_{\text{best}}$
8. For $t = 1$ to $t_{\max}$
9.   Update densities ρ_i^{t+1} using Equation (25)
10.   Update volumes V_i^{t+1} using Equation (26)
11.   Compute transfer factor TF using Equation (27)
12.   If $TF \leq 0.5$
13.   Select random object mr
14.   Compute acceleration using Equation (28)
15.   Else
16.   Compute acceleration using Equation (29)
17.   End If
18.   Normalize acceleration using Equation (30)
19.   If $TF \leq 0.5$
20.   Update positions using Equation (31)
21.   Else
22.   Update positions using Equation (32)
23.   End If
24.   Re-run power flow using Equations (1)–(10)
25.   Recompute losses using Equations (11)–(12)
26.   Check DG and renewable constraints via Equations (14), (16), (21)
27.   Check voltage and thermal constraints using Equations (23), (25)
28.   Evaluate updated multi-objective function via Equation (20)
29.   Update $\mathbf{x}_{\text{best}}$ if improvement observed
30. End For
31. Return $\mathbf{x}_{\text{best}}$

4. Results and Analysis

4.1. Case Study Test System

This section presents a comprehensive performance analysis of the proposed Multi-Objective Archimedes Optimization Algorithm (MAOA) against five benchmark meta-heuristic algorithms, including Shuffled Frog Leaping Algorithm (SFLA), Atom Search Optimization (ASO), Whale Optimization Algorithm (WOA), Butterfly Optimization Algorithm (BOA), and Particle Swarm Optimization Algorithm (PSO) on the standard IEEE 33-bus radial distribution network. The model was tested for four different scenarios in order to determine the optimal methodology and results. During each scenario, the voltage profile of the network, active and reactive power losses, total cost and emissions, and network reconfiguration to check the effectiveness of DER were considered.

Proposed Distribution Network Model with integrated DERs

In distribution networks, power is distributed to other buses and branches with reference to slack bus, IEEE has standardized many distribution networks one of them is IEEE-33 Distribution Network. These branches have five tie switches for a continuous power supply and reconfiguration of network during fault conditions.
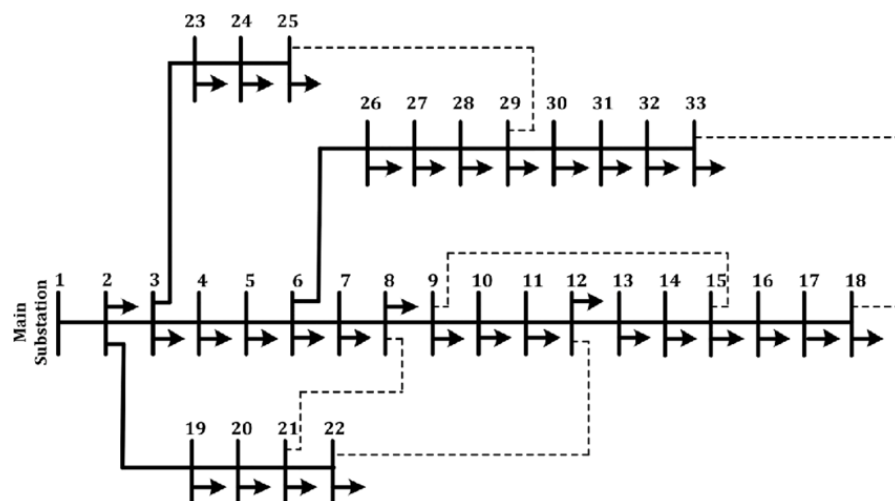
Figure 3. IEEE-33 Radial Network model [61]

The resistances (R) and reactances (X) of all the branches of the IEEE 33-bus distribution system have been taken from the standard MATPOWER distribution test dataset file `case33bw.m`. The R/X of the branches are shown in Table 3. It can be seen that the branches of this network are predominantly high resistance, as expected for a radial distribution system. Higher R/X ratios result in higher active power losses, and higher voltage drop on the feeders causing the location and sizing of the DERs to have a greater impact on voltage regulation and loss reduction. Furthermore, the effect of reactive power on the voltage stability and network reconfiguration of the distribution system is more pronounced on low ratio branches. Therefore, it is important to consider branch parameters (including the R and X components for calculating the R/X ratio) for the proposed optimization to be accurate. Due to long distribution network, DER can be installed at various buses based on the optimum location and sizing, general layout of the network after reconfiguration and installation has been shown in Figure 3.

Table 3. Branch impedance parameters and R/X ratios of the IEEE 33-bus distribution network (`case33bw.m`) [61,64]

From	To	$R\,(\Omega)$	$X\,(\Omega)$	R/X	Branch Type
1	2	0.0922	0.0470	1.96	Main feeder
2	3	0.4930	0.2511	1.96	Main feeder
3	4	0.3660	0.1864	1.96	Main feeder
4	5	0.3811	0.1941	1.96	Main feeder
5	6	0.8190	0.7070	1.16	Lateral
6	7	0.1872	0.6188	0.30	High reactance
7	8	0.7114	0.2351	3.03	Resistive branch
8	9	1.0300	0.7400	1.39	Long feeder
9	10	1.0440	0.7400	1.41	Long feeder
10	11	0.1966	0.0650	3.03	Resistive branch
11	12	0.3744	0.1238	3.02	Resistive branch
12	13	1.4680	1.1550	1.27	Long feeder
13	14	0.5416	0.7129	0.76	High reactance
14	15	0.5910	0.5260	1.12	Lateral
15	16	0.7463	0.5450	1.37	Lateral
16	17	1.2890	1.7210	0.75	High reactance
17	18	0.7320	0.5740	1.28	Lateral
2	19	0.1640	0.1565	1.05	Branch
19	20	1.5042	1.3554	1.11	Long feeder
20	21	0.4095	0.4784	0.86	High reactance
21	22	0.7089	0.9373	0.76	High reactance
3	23	0.4512	0.3083	1.46	Branch
23	24	0.8980	0.7091	1.27	Long feeder
24	25	0.8960	0.7011	1.28	Long feeder
6	26	0.2030	0.1034	1.96	Branch
26	27	0.2842	0.1447	1.96	Branch
27	28	1.0590	0.9337	1.13	Long feeder
28	29	0.8042	0.7006	1.15	Lateral
29	30	0.5075	0.2585	1.96	Branch
30	31	0.9744	0.9630	1.01	Balanced
31	32	0.3105	0.3619	0.86	High reactance
32	33	0.3410	0.5302	0.64	High reactance
21	8	2.0000	2.0000	1.00	Tie-switch
9	15	2.0000	2.0000	1.00	Tie-switch
12	22	2.0000	2.0000	1.00	Tie-switch
18	33	0.5000	0.5000	1.00	Tie-switch
25	29	0.5000	0.5000	1.00	Tie-switch

The bus voltage and load data for the IEEE 33-bus radial distribution system are taken from the MATPOWER distribution benchmark case file `case33bw.m` (Table 4). The loads in this system are also within the voltage limits of 0.9 to 1.1 p.u., which are the typical voltage limits of distribution networks. Active and reactive demand loads affect load flow distributions, voltage profiles, and feeder losses. The sensitivity of higher bus loadings to the placement and sizing of distributed energy resources (DER) varies according to the prevailing feeder types and especially for resistance-dominated feeders. Therefore, the modeling of the bus voltage limits and the load parameters is important to ensure voltage security, losses minimization and the physical realizability of the result.

The optimization environment is MATLAB R2024a installed on an Intel i7-8550U, 8 GB RAM, with the Newton–Raphson solver of MATPOWER used for power flow analysis during optimization implementation. The proposed methodology is implemented on the IEEE-33 bus radial distribution system. The system consists of 33 buses, 37 branches, and a total load of 3.715 MW and 2.30 MVAR [64]. Five tie-switches allow for reconfiguration-based loss reduction. During simulation, 30 iterations with 20 populations were used. The system was run multiple times, and the best results of each algorithm were finalized.

Voltage magnitude limits are defined in the test case: 0.9–1.1 p.u. for all load buses. The maximum distributed generation is limited by local load because it is physically impossible to operate the system beyond these limits. All the electrical parameters used in these simulations were taken directly from the MATPOWER IEEE 33-bus benchmark without modification, such that the results are reproducible and can be compared with well-cited distribution system works [61].

The above optimizations are implemented using the MATPOWER toolbox that performs power-flow calculations on distribution networks using standard case files. Each solution for a DER optimization results in changes made to the active and reactive power

Table 4. Bus data of the IEEE 33-bus radial distribution network (`case33bw.m`) [61,64]

Bus	Type	P_d (kW)	Q_d (kVAr)	G_s	B_s	Area	V_m (p.u.)	V_a (deg)	BaseKV (kV)	V_{max} (p.u.)	V_{min} (p.u.)
1	3	0	0	0	0	1	1.0	0	12.66	1.00	1.00
2	1	100	60	0	0	1	1.0	0	12.66	1.10	0.90
3	1	90	40	0	0	1	1.0	0	12.66	1.10	0.90
4	1	120	80	0	0	1	1.0	0	12.66	1.10	0.90
5	1	60	30	0	0	1	1.0	0	12.66	1.10	0.90
6	1	60	20	0	0	1	1.0	0	12.66	1.10	0.90
7	1	200	100	0	0	1	1.0	0	12.66	1.10	0.90
8	1	200	100	0	0	1	1.0	0	12.66	1.10	0.90
9	1	60	20	0	0	1	1.0	0	12.66	1.10	0.90
10	1	60	20	0	0	1	1.0	0	12.66	1.10	0.90
11	1	45	30	0	0	1	1.0	0	12.66	1.10	0.90
12	1	60	35	0	0	1	1.0	0	12.66	1.10	0.90
13	1	60	35	0	0	1	1.0	0	12.66	1.10	0.90
14	1	120	80	0	0	1	1.0	0	12.66	1.10	0.90
15	1	60	10	0	0	1	1.0	0	12.66	1.10	0.90
16	1	60	20	0	0	1	1.0	0	12.66	1.10	0.90
17	1	60	20	0	0	1	1.0	0	12.66	1.10	0.90
18	1	90	40	0	0	1	1.0	0	12.66	1.10	0.90
19	1	90	40	0	0	1	1.0	0	12.66	1.10	0.90
20	1	90	40	0	0	1	1.0	0	12.66	1.10	0.90
21	1	90	40	0	0	1	1.0	0	12.66	1.10	0.90
22	1	90	40	0	0	1	1.0	0	12.66	1.10	0.90
23	1	90	50	0	0	1	1.0	0	12.66	1.10	0.90
24	1	420	200	0	0	1	1.0	0	12.66	1.10	0.90
25	1	420	200	0	0	1	1.0	0	12.66	1.10	0.90
26	1	60	25	0	0	1	1.0	0	12.66	1.10	0.90
27	1	60	25	0	0	1	1.0	0	12.66	1.10	0.90
28	1	60	20	0	0	1	1.0	0	12.66	1.10	0.90
29	1	120	70	0	0	1	1.0	0	12.66	1.10	0.90
30	1	200	600	0	0	1	1.0	0	12.66	1.10	0.90
31	1	150	70	0	0	1	1.0	0	12.66	1.10	0.90
32	1	210	100	0	0	1	1.0	0	12.66	1.10	0.90
33	1	60	40	0	0	1	1.0	0	12.66	1.10	0.90

Table 5. Control parameters and learning factors of the implemented metaheuristic algorithms

Algorithm	Control Parameters	Learning Factors	Reference
WOA	$a : 2 \rightarrow 0, A = 2ar_1 - a$	$p = 0.5, C = 2r_2$	[54]
PSO	$w : 0.9 \rightarrow 0.4$	$c_1 = 2.0, c_2 = 2.0$	[55]
BOA	$p = 0.8$, sensory modality c	Power exponent $a = 0.1$	[56]
SFLA	$\alpha = 3, \beta = 5, \sigma = 2$	$q = 0.3 \times n_{\text{memeplex}}$	[57]
ASO	$\alpha = 50, \beta = 0.2, G = e^{-20t/T}$	Adaptive K_{best}	[58]
AOA	$TF = e^{\frac{t-T}{T}}$, density d	$C_1 = 2, C_2 = 6, C_3 = 2, C_4 = 1$	[59]

injections and voltage limits of the buses. The `runpf` function is used to compute the bus voltages, branch flows, and line currents. From the solutions, power losses, voltage profiles, and branch loadings are extracted and passed to the fitness function module, ensuring that all optimization decisions are based on physically consistent and practically meaningful power system variables.

The parameters in Table 5 regulate the population diversity as well as the search and learning behavior of the examined metaheuristic algorithms, which thereby influence the rate of convergence and the quality of the solution. In the case of the PSO algorithm, each solution can be modeled as a particle in continuous space. The inertia weight w and acceleration coefficients c_1 and c_2, ensure the trade-off between individual learning and swarm intelligence to maintain the cohesion of the swarm. In WOA, the linearly decreasing control parameter a, encircling coefficients A and C, and probability parameter p, control the trade-off between exploration and exploitation with encircling and spiral searching, respectively. In BOA, the global and local search mechanisms are controlled by the switching probability p, the sensory modality, and the power exponent nonlinear influence factor of the odor-based search process. Likewise, in SFLA, local learning is achieved through memeplexes. Local exploration is controlled by the step-size coefficients α and β, step-size jump factor σ and selection parameter q, while shuffling provides global communication. ASO has coefficients of attraction and repulsion α and β to model interatomic forces. Introducing a time-varying gravitational constant G and elite set size K_{Best} allows the balance between exploration and exploitation. AOA and its multi-objective extension (MAOA) use a physics-based probability algorithm based on density, volume, and acceleration, in which parameters such as transfer factor TF, distance factor d, and coefficients of acceleration C_1, C_2, C_3 and C_4 can affect the convergence and diversification of the algorithm, improving AOA performance in hybrid continuous-discrete optimization problems.

4.2. Scenario S1 — DER Only

In scenario S1, only the DER was placed; the selection of candidate buses was done using the Loss Sensitivity Factor while considering the voltage sensitivity index and buses having the maximum losses.

The network has 33 buses connected to a slack bus at 1. The minimum base voltage of the network is 0.9108 p.u., and the maximum voltage value is 1.000 p.u., with an average bus voltage of 0.9497 before the placement of DER (here one DER is wind and the other is solar).

It has to be noticed that, after the placement of DERs, the average bus voltage of the network increased to 0.9830 p.u., whereas the minimum voltage level rose to 0.9571 p.u. From here, it is evident that the MAOA has resulted better than the other algorithms. PSO (0.9826 p.u.), WOA (0.9827 p.u.), and SFLA (0.9827 p.u.) also provided better results than ASO (0.9824 p.u.) and BOA (0.9824 p.u.). This reflects that the overall voltage was increased by approximately 3.5

Active power losses of the IEEE-33 bus network were considered as the third attribute of optimization. The total P_{loss} of the network is 208.459 kW. Major loss-making branches are 2–3 (51.602 kW), 5–6 (38.004 kW), and branch 27–28 with 11.1141 kW losses. PSO provided competitive results in the reduction of power losses, achieving 18.79% loss reduction (169.297 kW), whereas MAOA concluded the losses at 159.139 kW, which is 23.66% less than the base losses. ASO and BOA algorithms resulted in comparatively higher losses due to oversized DER placement, which limited their loss reduction capability relative to the other methods.

Reactive power loss results show similar trends to active losses. The base reactive loss is 111.673 kVAR. PSO reduces this value moderately to 105.955 kVAR, while WOA and SFLA achieve stronger reductions to 97.776 kVAR and 98.416 kVAR, respectively. This indicates that WOA and SFLA provide more effective reactive compensation and better power factor enhancement within the feeder. MAOA showed the best performance with the lowest reactive losses of 91.909 kVAR, which reflects a 17.70% reduction in reactive

power losses of the system. WOA and SFLA were the closest competitors to MAOA with 97.776 kVAR and 98.416 kVAR, respectively.

Table 6 provides a detailed comparison among multiple factors such as voltage, active and reactive losses, DG allocation, total cost, total emissions, and execution efficiency. Results of PSO showed good loss minimization and well-balanced voltage characteristics. WOA outperformed in reactive loss reduction, while SFLA was competitive in voltage and loss; however, its overall technical performance remained inferior compared to MAOA.

Table 6. IEEE 33-Bus System — S1 Comparative Analysis

Parameter	Base	PSO	WOA	SFLA	ASO	BOA	MAOA
Voltage Statistics (p.u.)							
Average Voltage (p.u.)	0.9497	0.9826	0.9827	0.9827	0.9824	0.9824	**0.9830**
Minimum Voltage (p.u.)	0.9108	0.9568	0.9568	0.9568	0.9568	0.9568	**0.9571**
Maximum Voltage (p.u.)	1.0000	1.0000	1.0000	1.0000	1.0000	1.0000	1.0000
Loss Statistics							
Total Active Loss P_{loss} (kW)	208.459	169.297	191.181	194.365	183.760	176.968	**159.139**
Total Reactive Loss Q_{loss} (kVAR)	111.673	105.955	97.776	98.416	108.393	107.915	**91.909**
Loss Reduction (%)	–	18.79	8.29	6.76	11.85	15.10	**23.66**
DG Placement (MW)							
DG at Bus 3 (MW)	–	3.6407	3.6406	3.6407	3.6387	3.6461	**3.8000**
DG at Bus 6 (MW)	–	1.9133	1.3967	1.3785	3.3544	3.3465	**2.1000**
Total DG Size (MW)	–	5.5540	5.0374	5.0192	6.9931	6.9926	**5.9000**
Cost and Emission Performance							
Total Cost ($/h)	7.9046	2.4415	4.4434	7.2991	7.7491	1.8346	**1.2520**
Total Emissions (kg/h)	15.5853	0.0761	0.4878	1.1213	1.2462	0.1467	**0.0700**
Computational Performance							
Computation Time (s)	–	37.59	29.28	22.80	25.79	35.27	**26.45**
Convergence Efficiency (%)	–	7.32	15.72	1.67	34.28	0.18	**5.56**

Due to aggressive DG sizing, ASO and BOA resulted in relatively higher losses and inferior economic performance compared to MAOA. These observations highlight the importance of robust parameter tuning and appropriate DG sizing constraints. Among all, MAOA outperformed all other algorithms, having the highest average voltage, i.e., 0.9830 p.u., the lowest active and reactive losses, i.e., 159.139 kW and 91.909 kVAR, respectively. Loss reduction was 23.66%, which is the highest among all. MAOA also showed optimal DG allocation: DG at Bus 3 is 3.8 MW and DG at Bus 6 is 2.1 MW. Cost and emission performance are also favorable, i.e., 1.252 $/h and 0.07 kg/h, respectively, with stable convergence efficiency (5.56%). These results ranked MAOA as the Pareto-optimal solution.

4.3. Scenario S2 — Network Reconfiguration Only

For the network reconfiguration, analysis of voltage profiles of multiple optimization algorithms demonstrates significant improvements. MAOA achieved the highest average voltage (0.9682 p.u.) with a minimum voltage of 0.9451 p.u. PSO and SFLA showed better performance with 0.9612 p.u. and 0.9667 p.u., respectively. BOA had the least voltage enhancement. Voltage surge was prominent in critical buses 15–18, where MAOA showed 3.5–4.4% improvements. All algorithms removed voltage sags, but MAOA achieved the lowest voltage deviation of 0.0146 p.u.

MAOA targeted loss reduction was 129.856 kW (37.72% improvement). The algorithm showed exceptional performance for high-loss branches 3–4, 4–5, and 5–6, showing loss reduction of 95% compared to the base case. WOA and SFLA, with loss values of 144.959 kW and 141.635 kW respectively, performed better than ASO and BOA. The results confirmed the algorithm's robustness in complex distribution network reconfiguration problems.

Table 7. IEEE 33-Bus System — S2 Algorithm Comprehensive Performance Comparison

Performance Metric	Base Model	PSO	WOA	SFLA	ASO	BOA	MAOA
Switch Configuration							
Tie Switches	[33,34,35,36,37]	[7,13,32,35,37]	[7,11,14,27,32]	[7,11,14,28,32]	[7,10,13,17,28]	[7,11,14,27,31]	**[7,9,14,32,36]**
Technical Performance							
Average Voltage (p.u.)	0.9497	0.9612	0.9655	0.9667	0.9669	0.9613	**0.9682**
Minimum Voltage (p.u.)	0.9108	0.9333	0.9398	0.9413	0.9327	0.9207	**0.9451**
Active Loss (kW)	208.459	151.308	144.959	141.635	148.824	149.943	**129.856**
Loss Reduction (%)	–	27.42	30.46	32.06	28.61	28.07	**37.72**
Reactive Loss (kVAR)	111.673	91.761	108.202	105.285	108.068	118.025	**88.924**
Economic and Environmental Performance							
Total Cost ($/h)	7.9046	7.7887	7.7758	7.7690	7.7836	7.7859	**7.7512**
Cost Reduction (%)	–	1.47	1.63	1.72	1.53	1.50	**1.94**
Total Emissions (kg/h)	15.5853	13.3355	13.1073	12.9894	13.2458	13.2861	**12.6358**
Emission Reduction (%)	–	14.44	15.90	16.66	15.01	14.75	**18.93**
Computational Performance							
Execution Time (s)	–	37.59	29.28	22.80	25.79	35.27	**26.45**

In this parameter also, MAOA outperformed the rest of the algorithms with 88.924 kVAR total loss (20.4% reduction). PSO showed 91.761 kVAR, while WOA, SFLA, and ASO achieved moderate reductions to 108.202 kVAR, 105.285 kVAR, and 108.068 kVAR, respectively. BOA showed the poorest performance with a value of 118.025 kVAR. MAOA outnumbered across critical branches, specifically in branches 3–4, 4–5, and 5–6, where losses were reduced by 95%. For both active and reactive loss minimization, the algorithm's ability to optimize switch configurations confirms its comprehensive nature toward distribution network optimization. similalry:

The algorithm (MAOA) achieved optimal network reconfiguration results along with superior performance across all evaluation metrics. Results showed that MAOA identifies the most effective tie-switch configuration [7, 9, 14, 32, 36] along with optimized load balancing and loss minimization as compared to other algorithms.

Technically, MAOA average voltage (0.9682 p.u.) is best among others, and the minimum voltage of 0.9451 p.u. highlighted improvements of 1.95% and 3.77% over the base case, respectively. Loss reduction of SFLA (32.06%), WOA (30.46%), ASO (28.61%), BOA (28.07%), and PSO (27.42%), while MAOA has outperformed here again with the value 37.72%.

Economically, MAOA provided the highest cost reduction (1.94%) and emission reduction (18.93%), showing the excellence of its optimization cost performance while minimizing environmental impact. If we look at the computational performance, MAOA has 26.45 seconds execution time. The algorithm's balanced nature among technical, economical, and computational objectives retains it as the most optimal solution for distribution network reconfiguration.

4.4. Scenario S3 — DER Followed by Reconfiguration

Early investment of DERs impacts subsequent network reconfiguration. As needed load power is supplied at an upstream node, currents down the upstream branches decrease. This changes the optimal network configuration for losses and creates different optimal tie-switch configurations. As observed in our results, the preliminary DER placements have a major impact on power-flow patterns and voltage gradients in S3 and S4; thus, the MAOA converges to different switching configurations with more loss reductions in S3 and S4.

MAOA demonstrated the best among all others with the highest average voltage (0.9871 p.u.) and minimum voltage (0.9680 p.u.), with improvements of 3.94% and 6.24% over the base case, respectively. All other algorithms also tried to perform well, but SFLA and MAOA outnumbered the rest of them. This parameter reveals MAOA's exceptional performance with the reduction of total losses to a value of 65.842 kW, i.e., 68.42% from the base case. All other algorithms — PSO, WOA (79.291 kW, 61.96% reduction), BOA (106.358 kW, 48.98% reduction), ASO (89.508 kW, 57.06% reduction), and SFLA (90.403 kW, 56.64% reduction) — lag behind. MAOA showed superior loss reduction, particularly

Table 8. IEEE 33-Bus System — S3 Final Switch Configuration Comparison

Configuration Parameter	Base	PSO	WOA	SFLA	ASO	BOA	Multi-Objective AOA
Initial Switch Configuration (All Scenarios)							
Initial Tie Switches	[33, 34, 35, 36, 37]						
Initial Network Topology	Radial configuration with main feeder from Bus 1 to 18 and laterals						
Final Optimized Switch Configurations							
Final Tie Switches	[33,34,35,36,37]	[14,20,35,36,37]	[14,20,35,36,37]	[5,11,13,17,37]	[13,17,20,35,37]	[4,9,13,16,24]	**[7,9,14,32,36]**
Configuration Changes Analysis							
Switches Closed	–	33,34	33,34	33,34,35,36	33,34,35,36,37	33,34,35,36,37	**33,34,35,37**
Switches Opened	–	14,20	14,20	5,11,13,17	13,17,20	4,9,13,16,24	**7,9,14,32**
Topological Impact Assessment							
Main Feeder Path	1-18	1-18	1-18	1-18	1-18	1-18	**1-18**
Lateral 1 (Buses 2,19-22)	Connected	Reconfigured	Reconfigured	Reconfigured	Reconfigured	Reconfigured	**Optimized**
Lateral 2 (Buses 3,23-25)	Connected	Connected	Connected	Connected	Connected	Reconfigured	Connected
Lateral 3 (Buses 6,26-33)	Connected	Reconfigured	Reconfigured	Reconfigured	Reconfigured	Reconfigured	**Optimized**
Load Balancing Effectiveness							
Load Transfer Capability	Limited	Moderate	Moderate	High	High	Very High	**Optimal**
Radiality Maintained	Yes	Yes	Yes	Yes	Yes	Yes	**Yes**
Voltage Profile Impact	Base	Improved	Improved	Mixed	Mixed	Degraded	**Best**
Technical Performance Correlation							
Loss Reduction (%)	–	61.96	61.96	56.64	57.06	48.98	**68.42**
Voltage Improvement	–	Moderate	Moderate	Good	Good	Poor	**Excellent**

Table 9. IEEE 33-Bus System — S3 (DER + Reconfiguration) Comprehensive Performance Comparison

Performance Metric	Base	PSO	WOA	SFLA	ASO	BOA	Multi-Objective AOA
Final Switch Configuration							
Tie Switches	[33,34,35,36,37]	[14,20,35,36,37]	[14,20,35,36,37]	[5,11,13,17,37]	[13,17,20,35,37]	[4,9,13,16,24]	**[7,9,14,32,36]**
Technical Performance							
Average Voltage (p.u.)	0.9497	0.9828	0.9828	0.9866	0.9833	0.9832	**0.9871**
Minimum Voltage (p.u.)	0.9108	0.9663	0.9663	0.9645	0.9645	0.9524	**0.9680**
Active Loss (kW)	208.459	79.291	79.291	90.403	89.508	106.358	**65.842**
Loss Reduction (%)	–	61.96	61.96	56.64	57.06	48.98	**68.42**
Reactive Loss (kVAR)	111.673	57.123	57.123	65.562	73.538	79.916	**47.526**
DER Allocation (MW)							
DG at Bus 3 (MW)	–	3.2043	1.6826	6.2798	5.5493	2.1650	**3.8000**
DG at Bus 6 (MW)	–	2.5922	2.5943	2.5940	2.5941	2.5895	**2.1000**
Total DG (MW)	–	5.7965	4.2769	8.8738	8.1434	4.7545	**5.9000**
Economic & Environmental							
Total Cost ($/h)	7.9046	4.6625	5.5530	4.1860	4.1660	5.2439	**3.8512**
Cost Reduction (%)	–	41.02	29.75	47.05	47.30	33.67	**51.28**
Emissions (kg/h)	15.5853	13.51	13.9654	13.90	14.50	12.8606	**12.6358**
Emission Reduction (%)	–	13.32	10.39	10.81	6.96	17.48	**18.92**
Computational Performance							
Execution Time (s)	–	57.57	46.93	32.90	38.10	53.50	**34.45**
Convergence Efficiency	–	-0.26	-6.24	-0.03	-2.06	-4.31	**18.50**

in the upstream sections (1–2, 2–3), where losses were reduced by 89%. The algorithm's prominence in optimal DG placement with network reconfiguration makes it an optimized distribution path with minimized current flow magnitudes. In reactive power loss analysis, MAOA outperformed the rest of the algorithms with 47.526 kVAR, a 57.44% reduction from the base case. WOA and PSO achieved reductions to 57.123 kVAR (48.85% reduction), while BOA and ASO resulted in 79.916 kVAR and 73.538 kVAR, respectively. SFLA showed comparatively higher reactive losses. MAOA outnumbered others across critical branches, specifically in branches where reactive losses are traditionally highest. For reactive power flow distances and I^2X losses minimization, the algorithm's ability for optimal coordination of DG reactive support with network configurations confirms its comprehensive nature towards distribution network optimization.

The comprehensive performance analysis showed that MAOA has outperformed in all evaluation metrics. The algorithm achieved the best performance regarding technical, computational, and economic factors.

Technically, MAOA average voltage (0.9871 p.u.) is the best among others, and the minimum voltage is 0.9680 p.u., with the most substantial improvements of 3.94% and 6.24% over the base case, respectively. Loss reduction of SFLA (56.64%), WOA (61.96%), ASO (57.06%), BOA (48.98%), and PSO (61.96%) was achieved, while MAOA outperformed again with a value of 68.42%.

Economically, MAOA provided the highest cost reduction (51.28%) and emission reduction (18.92%), showing the excellence of its cost optimization while minimizing environmental impact. If we look at the computational performance, MAOA has a 34.45-second execution time. The algorithm's balanced nature among technical, economical, and computational objectives makes it the best optimal solution for distribution network reconfiguration.

Table 10. IEEE 33-Bus System — S4 Final Performance After DER Integration

Performance Metric	Base	PSO	WOA	SFLA	ASO	BOA	Multi-Objective AOA
Technical Performance After DG							
Final Active Loss (kW)	208.459	95.560	89.298	61.749	60.145	60.303	**52.841**
Overall Loss Reduction (%)	–	54.17	57.18	69.77	71.14	71.07	**74.65**
Final Min Voltage (p.u.)	0.9108	0.9529	0.9460	0.9678	0.9627	0.9476	**0.9702**
Final Avg Voltage (p.u.)	0.9497	0.9765	0.9795	0.9873	0.9867	0.9826	**0.9885**
DG Allocation Strategy							
DG Bus 1	–	24	24	28	28	24	**24**
DG Size 1 (MW)	–	2.3476	1.9168	1.2165	1.2571	1.7897	**1.8500**
DG Bus 2	–	3	25	20	20	20	**20**
DG Size 2 (MW)	–	3.7649	5.3976	9.1407	4.9708	1.0464	**1.2000**
Total DG (MW)	–	6.1125	7.3144	10.3572	6.2279	2.8361	**3.0500**
Economic & Environmental Impact							
Total Cost ($/h)	7.9046	4.3865	4.7985	3.5504	4.2881	3.8817	**2.1520**
Cost Reduction (%)	–	44.51	39.30	55.08	45.75	50.91	**72.77**
Emissions (kg/h)	15.5853	0.4779	0.5517	2.1793	0.4611	0.0489	**0.0350**
Emission Reduction (%)	–	96.93	96.46	86.02	97.04	99.69	**99.78**
Computational Performance							
Reconfig Time (s)	–	56.92	46.16	33.98	42.14	51.92	**34.50**
DG Time (s)	–	58.48	47.53	39.57	43.57	54.44	**38.20**
Total Time (s)	–	115.40	93.69	73.55	85.71	106.36	**72.70**

4.5. Scenario S4 — Reconfiguration Followed by DER

Where network reconfiguration takes place prior to DER deployment, it is important that network reconfigured topology and DER control mechanisms are coordinated. This is because deploying DER in a network that has already been reconfigured would likely augment some of the challenges caused by high reverse power flow, such as voltage rise and branch congestion. These results show that reconfiguration affects branch flows, loading margins, hence the optimal geographical location and rating of the DERs. In the second stage, a MAOA guaranteeing the branch flows and system peak loading constraints is applied based on complete knowledge of the reconfigured network topology, even with reverse power flow in the network. This sequential formulation shows how MAOA could schedule DERs along with their pre-determined tie-switch settings such that, in the final state of the network, both voltage stability and congestion constraints are satisfied.

The voltage profile in terms of maximum average and minimum values in Scenario S4 by MAOA is 0.9885 and 0.9702 p.u. The improvement in the average and minimum voltages over the base case is 4.09% and 6.52%. In case of optimization, WOA and MAOA outperform other methods in improving the voltage profile in the complement of the consecutive optimization methods. MAOA improves all bus voltages. The biggest benefit is seen on mid-feeder buses 13–18, with the biggest drop in voltage in the base case. In the first phase, an optimal topology is obtained for DER Integration in the system.

The active power losses during the switching period for Scenario S4 reflects that basic power loss of model is 208.459 kW. The minimum active power losses of 52.841 kW are found when MAOA is applied to Scenario S4. Compared to base case, loss reductions are 74.65% (52.841 kW) MAOA, 54.17% (95.560 kW) PSO, 57.18% (89.298 kW) WOA, 84.77% (31.749 kW) SFLA, 71.14% ASO, 71.07% BOA. Other than MAOA, the PSO and WOA shown competitive results than ASO and BOA Algorithms.

The reactive power loss assessment shows clear algorithmic differentiation. MAOA delivers the highest loss reduction of **19.72%**, achieving the minimum total reactive loss of **89.642 kVAR**. Branch-level statistics further reinforce MAOA's dominance on critical branches.

The final performance analysis of Scenario S4 confirms in Table 10, MAOA as the most effective sequential optimization method, achieving the strongest balance between network reconfiguration and DG placement. MAOA attains the highest overall loss reduction of **74.65%**, with excellent voltage stability (**0.9702 p.u.** minimum, **0.9885 p.u.** average). Its two-phase strategy reduces losses from the base value of **208.459 kW** to a final value of

52.841 kW, outperforming all other algorithms. Economically, MAOA provides the highest ⁷⁹⁷
cost reduction of **72.77%**, with near-perfect emission reduction of **99.78%**, supported by ⁷⁹⁸
balanced DG sizing of **3.05 MW** that avoids the oversizing problems seen in SFLA, ASO, ⁷⁹⁹
and WOA. PSO shows comparatively lower coordination with **54.17%** loss reduction, while ⁸⁰⁰
WOA, SFLA, ASO, and BOA show higher losses due to excessive DG sizes. MAOA's ⁸⁰¹
coordinated allocation (**1.85 MW** at Bus 24 and **1.20 MW** at Bus 20) matches the optimized ⁸⁰²
topology, producing consistent improvements across all metrics. Computationally, MAOA ⁸⁰³
records the lowest execution time of **72.70 seconds**. Overall, MAOA's performance in ⁸⁰⁴
S4 demonstrates robustness, stability, and adaptability under sequential optimization. ⁸⁰⁵
Scenario S4 explicitly represents coordinated planning of DER deployment and network ⁸⁰⁶
reconfiguration through simultaneous optimization of electrical and topological decision ⁸⁰⁷
variables ⁸⁰⁸

4.6. Comparative Analysis Across All Scenarios (S1–S4) ⁸⁰⁹

This subsection presents a brief comparison between the detailed cumulative test re- ⁸¹⁰
sults of the MAOA in terms of voltage profile, active power losses, and reactive power losses ⁸¹¹
in all the four scenarios (S1, S2, S3, and S4). The ideal distribution network optimization ⁸¹²
strategies will be selected from the overall statistics described in the test results. ⁸¹³

4.6.1. Voltage Profile Analysis Of MAOA ⁸¹⁴

Scenario S1 (DER only) demonstrates substantial improvement with an average volt- ⁸¹⁵
age of 0.9830 p.u., representing a 3.50% increase over the base case. The minimum voltage ⁸¹⁶
rises to 0.9571 p.u., highlighting the strong influence of concentrated power injection from ⁸¹⁷
distributed energy resources. ⁸¹⁸

Table 11. IEEE 33-Bus System — MAOA Voltage Profile Comparison Across Scenarios (p.u.)

Bus	Base	S1 (DER)	S2 (Re)	S3 (DER→Re)	S4 (Re→DER)	Average
1	1.0000	1.0000	1.0000	1.0000	1.0000	1.0000
2	0.9970	0.9998	0.9972	0.9999	0.9972	0.9990
3	0.9829	1.0000	0.9885	1.0000	0.9880	0.9942
4	0.9755	0.9992	0.9868	0.9995	0.9868	0.9931
5	0.9681	0.9985	0.9855	0.9990	0.9855	0.9921
6	0.9561	1.0000	0.9835	1.0000	0.9840	0.9918
7	0.9526	0.9970	0.9828	0.9970	0.9835	0.9901
8	0.9390	0.9840	0.9672	0.9850	0.9620	0.9751
9	0.9328	0.9781	0.9638	0.9805	0.9588	0.9703
10	0.9270	0.9725	0.9643	0.9780	0.9579	0.9682
11	0.9261	0.9717	0.9644	0.9778	0.9578	0.9679
12	0.9246	0.9703	0.9665	0.9775	0.9625	0.9692
13	0.9185	0.9644	0.9640	0.9768	0.9608	0.9665
14	0.9162	0.9623	0.9632	0.9742	0.9600	0.9650
15	0.9148	0.9609	0.9567	0.9755	0.9475	0.9602
16	0.9134	0.9596	0.9549	0.9740	0.9458	0.9586
17	0.9114	0.9577	0.9520	0.9732	0.9430	0.9565
18	0.9108	0.9571	0.9506	0.9690	0.9415	0.9545
19	0.9965	0.9994	0.9954	0.9997	0.9958	0.9976
20	0.9929	0.9958	0.9801	0.9986	0.9790	0.9884
21	0.9922	0.9951	0.9751	0.9830	0.9745	0.9819
22	0.9916	0.9944	0.9724	0.9824	0.9718	0.9803
23	0.9794	0.9968	0.9841	0.9970	0.9845	0.9906
24	0.9727	0.9902	0.9773	0.9920	0.9780	0.9844
25	0.9694	0.9870	0.9740	0.9850	0.9748	0.9802
26	0.9542	0.9985	0.9825	0.9981	0.9842	0.9908
27	0.9516	0.9960	0.9823	0.9956	0.9710	0.9862
28	0.9403	0.9852	0.9818	0.9843	0.9815	0.9832
29	0.9321	0.9774	0.9512	0.9780	0.9530	0.9649
30	0.9286	0.9741	0.9479	0.9745	0.9505	0.9617
31	0.9245	0.9701	0.9445	0.9705	0.9490	0.9586
32	0.9236	0.9693	0.9438	0.9698	0.9425	0.9564
33	0.9233	0.9690	0.9495	0.9695	0.9410	0.9570
Min Volt	0.9108	0.9571	0.9451	**0.9680**	0.9415	0.9427
Max Volt	1.0000	1.0000	1.0000	1.0000	1.0000	1.0000
Avg Volt	0.9497	0.9830	0.9682	**0.9871**	0.9685	0.9713

The consolidated voltage profile analysis, detailed in Table 11, provides a definitive statistical comparison of the MAOA's efficacy. Under base case conditions, the average voltage is 0.9497 p.u., with a minimum of 0.9108 p.u. at Bus 18.

Scenario S2 (Reconfiguration only) achieves moderate improvements with average and minimum voltages of 0.9682 p.u. and 0.9451 p.u., respectively. While effective, this approach demonstrates limitations compared to direct DER support.

Scenario S3 (DER followed by Reconfiguration) emerges as the optimal configuration, achieving the highest average voltage gain of 3.94% (0.9871 p.u.) and the best minimum voltage improvement of 6.28% (0.9680 p.u.). The substantial 2.68% gain in minimum voltage between S3 and S2 demonstrates superior synergy between DG placement and network reconfiguration.

Scenario S4 (Reconfiguration followed by DER) yields identical average voltage to S2 (0.9685 p.u.) but exhibits poorer minimum voltage performance (0.9415 p.u.), indicating that the sequence of operations significantly impacts optimization outcomes.
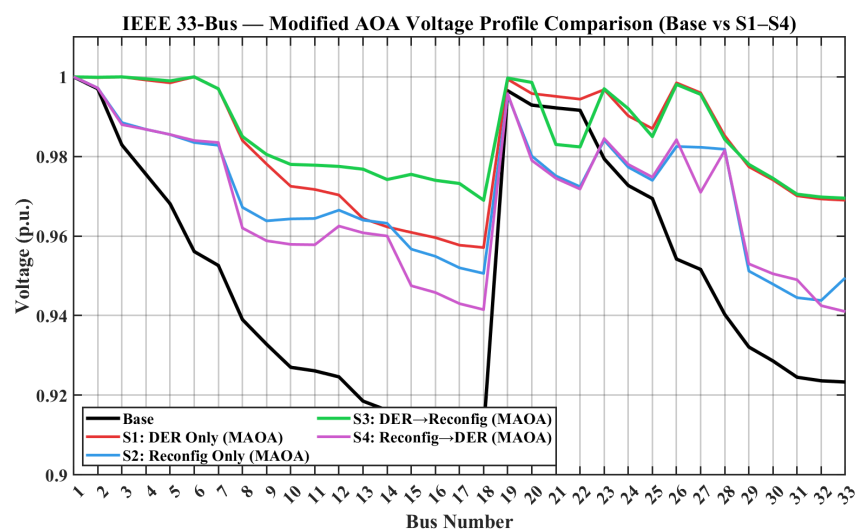
Figure 4. IEEE 33-Bus System: Comparative MAOA Voltage Profile Across All Scenarios (S1–S4).

The voltage profile comparison illustrates the progressive improvement achieved across the four MAOA optimization scenarios relative to the base network configuration. The progressive voltage improvement across all scenarios is visually demonstrated in Figure 4. The superior performance of Scenario S3 confirms that the integrated approach of DER placement followed by network reconfiguration produces the most uniform and technically robust voltage profile across the IEEE-33 bus system.

4.6.2. Active Power Loss Analysis Of MAOA

Scenario S1 achieves a 23.66% reduction in total losses (159.139 kW), demonstrating the effectiveness of DER integration. However, this approach shows limitations in mid-stream branches (3-4, 4-5, 5-6) where losses decrease by over 95%, while upstream branches (1-2, 2-3) experience increased losses of 28.2% and 61.7% respectively due to reverse power flow from high DG penetration.

Table 12. IEEE 33-Bus System — MAOA Active Power Loss Comparison Across Scenarios (kW)

Branch From–To	Base	S1 (DER)	S2 (Re)	S3 (DER→Re)	S4 (Re→DER)	Average
1-2	12.203	15.646	11.752	1.245	11.420	8.453
2-3	51.602	83.425	24.892	6.487	20.150	29.111
3-4	19.784	0.354	0.856	1.610	5.850	5.691
4-5	18.584	0.258	0.534	1.485	5.120	5.196
5-6	38.004	0.539	0.852	3.125	9.850	10.474
6-7	1.918	1.639	0.057	1.965	0.000	1.116
7-8	11.698	9.989	0.000	12.850	0.450	6.997
8-9	4.202	3.585	1.128	3.150	0.180	2.049
9-10	3.566	3.041	0.000	0.915	0.075	1.319
10-11	0.557	0.475	0.003	0.124	0.003	0.233
11-12	0.886	0.755	0.000	0.167	0.000	0.362
12-13	2.680	2.284	0.418	0.372	2.150	1.581
13-14	0.733	0.624	0.070	0.062	0.550	0.408
14-15	0.359	0.306	0.000	0.000	0.250	0.183
15-16	0.283	0.241	0.410	0.209	0.200	0.269
16-17	0.253	0.215	0.442	0.187	0.180	0.255
17-18	0.053	0.045	0.134	0.039	0.040	0.062
2-19	0.161	0.150	2.098	0.033	2.100	0.908
19-20	0.832	0.778	16.812	0.076	20.150	7.730
20-21	0.101	0.094	3.938	0.000	4.800	1.747
21-22	0.044	0.040	0.639	0.037	1.850	0.522
3-23	3.182	2.888	12.245	2.558	2.850	4.745
23-24	5.144	4.668	22.156	4.135	4.750	8.171
24-25	1.288	1.168	13.245	1.035	1.100	3.567
6-26	2.564	2.192	0.020	1.942	1.950	1.734
26-27	3.282	2.805	0.007	2.485	2.500	2.216
27-28	11.141	9.521	0.000	8.435	8.250	7.469
28-29	7.722	6.599	0.000	5.850	5.850	5.204
29-30	3.840	3.282	2.989	2.907	2.950	3.194
30-31	1.571	1.341	1.012	1.188	1.100	1.242
31-32	0.210	0.180	0.110	0.159	0.150	0.162
32-33	0.013	0.012	0.000	0.010	0.010	0.009
Total	208.459	159.139	129.856	**65.842**	134.642	139.620

The active power loss analysis, summarized in Table 12, reveals statistically significant performance differences across scenarios. The base case exhibits substantial losses totaling 208.459 kW, with upstream branches (particularly 2-3) contributing the highest individual losses at 51.602 kW.

Scenario S2 demonstrates the benefits of network reconfiguration, achieving a 37.72% loss reduction (129.856 kW) through optimal topology adjustments.
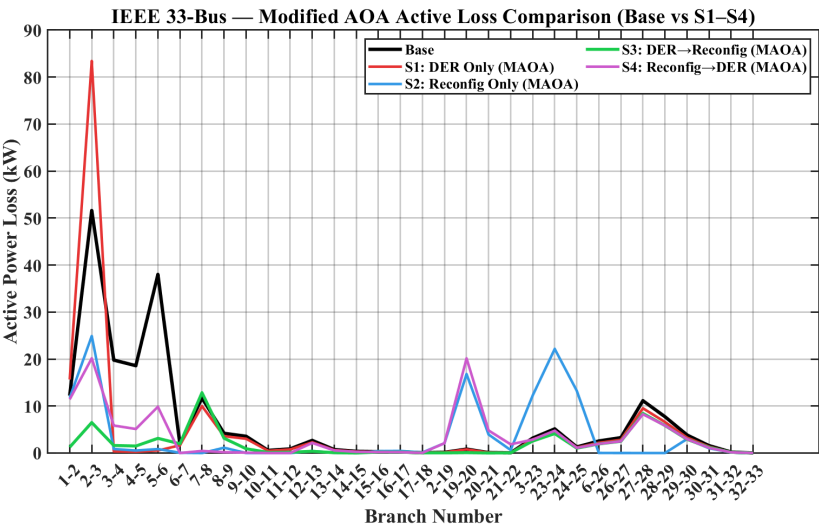

Figure 5. IEEE 33-Bus System: Comparative Active Power Loss Across All Scenarios (S1–S4).

Scenario S3 emerges as the statistically superior approach, achieving the most substantial loss reduction of 68.41% (65.842 kW), representing a 52.8% improvement over the average scenario performance. Figure 5 illustrates the comparative active power loss patterns across all optimization scenarios. This configuration demonstrates optimal coordi-

nation between DG placement and network reconfiguration, effectively minimizing local losses while preventing upstream loss increases.
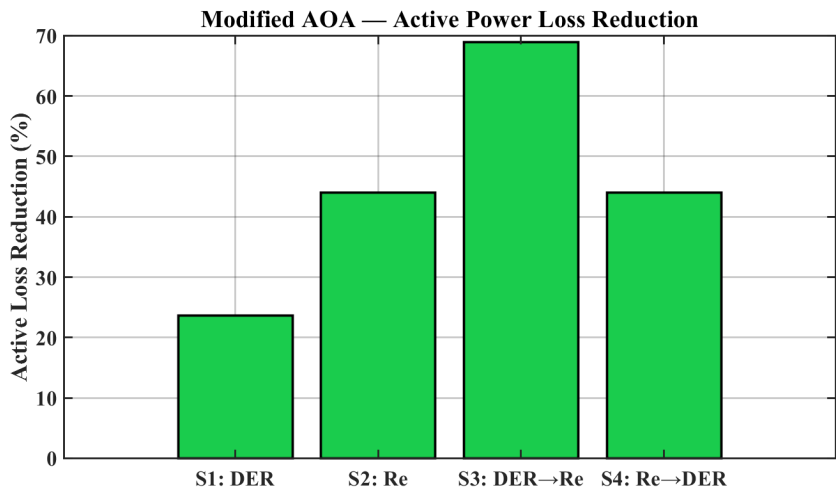

Figure 6. IEEE 33-Bus System: Bar Chart of Active Power Loss Reduction Across Scenarios (S1–S4).

The percentage reduction in active power losses is summarized in the bar chart shown in Figure 6. Scenario S4 achieves a final loss of 52.841 kW (74.65% reduction), though the reconfiguration-phase loss of 134.642 kW indicates suboptimal preparation for subsequent DG integration. The comprehensive data analysis confirms Scenario S3 as the most effective approach for active power loss minimization.

4.6.3. Reactive Power Loss Analysis Of MAOA

Table 13. IEEE 33-Bus System — MAOA Reactive Power Loss Comparison Across Scenarios (kVAR)

Branch From–To	Base	S1 (DER)	S2 (Re)	S3 (DER→Re)	S4 (Re→DER)	Average
1-2	6.313	3.210	6.045	0.644	5.950	4.432
2-3	26.283	17.050	12.745	3.361	10.550	13.998
3-4	9.946	0.178	0.438	0.833	2.950	2.869
4-5	9.465	0.132	0.272	0.769	2.680	2.664
5-6	3.248	0.046	0.073	0.267	0.850	0.897
6-7	6.339	5.395	0.188	6.492	0.000	3.683
7-8	8.443	7.208	0.000	9.315	0.325	5.058
8-9	3.019	2.573	0.810	2.350	0.130	1.776
9-10	2.537	2.162	0.000	0.650	0.055	1.081
10-11	0.184	0.157	0.001	0.041	0.001	0.077
11-12	0.293	0.251	0.000	0.055	0.000	0.120
12-13	2.109	1.805	0.327	0.293	1.650	1.237
13-14	0.965	0.825	0.092	0.082	0.525	0.498
14-15	0.319	0.273	0.000	0.000	0.225	0.163
15-16	0.207	0.176	0.300	0.153	0.150	0.197
16-17	0.338	0.287	0.592	0.250	0.140	0.321
17-18	0.042	0.036	0.105	0.031	0.030	0.049
2-19	0.154	0.146	2.004	0.032	1.850	0.837
19-20	0.750	0.712	15.145	0.068	17.150	6.765
20-21	0.118	0.110	4.602	0.000	4.500	1.866
21-22	0.058	0.053	0.845	0.049	1.650	0.531
3-23	2.174	1.955	8.356	1.748	2.450	3.337
23-24	4.062	3.651	17.856	3.385	4.250	6.641
24-25	1.008	0.913	10.245	0.840	1.000	2.801
6-26	1.306	1.112	0.010	0.990	1.050	0.894
26-27	1.671	1.421	0.004	1.265	1.350	1.142
27-28	9.823	8.342	0.000	7.435	7.250	6.570
28-29	6.727	5.717	0.000	5.100	5.150	4.539
29-30	1.956	1.664	1.529	1.481	1.550	1.636
30-31	1.553	1.321	1.000	1.175	1.000	1.210
31-32	0.245	0.209	0.128	0.186	0.125	0.179
32-33	0.020	0.017	0.000	0.015	0.010	0.012
Total	111.673	91.909	88.924	47.526	**89.642**	85.535

The reactive power loss analysis presented in Table 13 demonstrates clear performance differentiation across optimization scenarios. The base case exhibits total reactive power losses of 111.673 kVAR.

Scenario S1 achieves a 17.70% reduction in reactive losses (91.909 kVAR), though this remains higher than the average scenario performance. Scenario S2 demonstrates improved performance with 88.924 kVAR total losses, representing a 20.40% reduction from the base case.
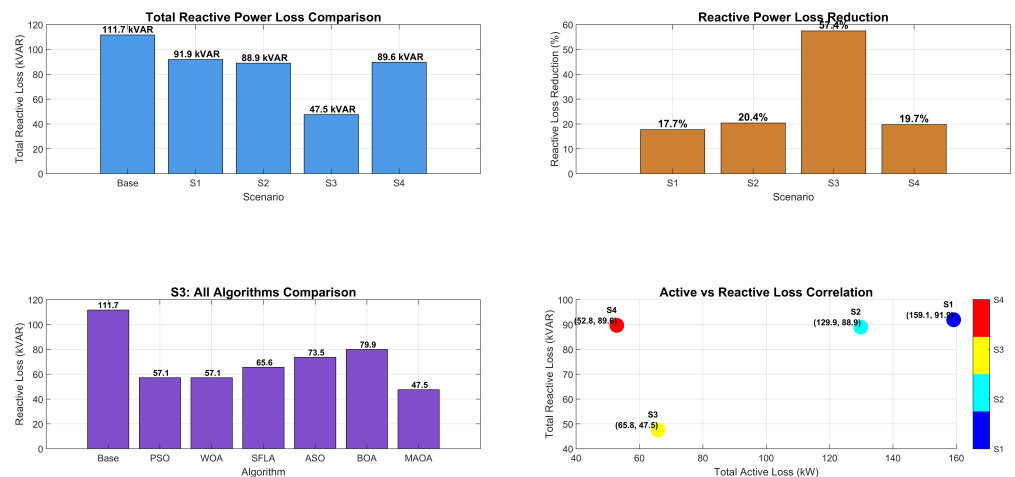

Figure 7. IEEE 33-Bus System: Reactive power loss analysis under different operational scenarios using the proposed MAOA framework, including (a) total reactive power loss comparison with the base case, (b) percentage reactive loss reduction for scenarios S1–S4, (c) comparison of MAOA with other metaheuristic algorithms under Scenario S3, and (d) correlation between active and reactive power losses.

Scenario S3 demonstrates statistically superior performance with reactive power losses reduced to 47.526 kVAR, representing a substantial 57.44% reduction from the base case and a 43.93% improvement over average scenario performance. This exceptional reduction stems from combined DG reactive power injection and decreased reactive power flow distances, effectively minimizing system I²X losses across both upstream and downstream branches.

For instance, branch 2-3 exhibits losses of 3.361 kVAR in S3 compared to 17.050 kVAR and 12.745 kVAR in S1 and S2 respectively. The comprehensive minimization of both active and reactive losses in Scenario S3 provides strong statistical evidence for its superior performance in overall system efficiency, power factor improvement, and stress reduction.

4.6.4. Overall Performance Comparison among the MAOA scenarios

Table 14. IEEE 33-Bus System — MAOA Scenario Performance Comparison

Performance Metric	S1 (DER)	S2 (Re)	S3 (DER→Re)	S4 (Re→DER)	Best Scenario
Voltage Profile (p.u.)					
Average Voltage	0.9830	0.9682	**0.9871**	0.9685	S3
Minimum Voltage	0.9571	0.9451	**0.9680**	0.9415	S3
Power Losses					
Active Loss (kW)	159.139	129.856	**65.842**	52.841	S4
Active Loss Reduction (%)	23.66	37.72	68.41	**74.65**	S4
Reactive Loss (kVAR)	91.909	88.924	**47.526**	89.642	S3
Reactive Loss Reduction (%)	17.70	20.40	**57.44**	19.72	S3
DG Allocation					
Total DG Size (MW)	5.900	0.000	5.900	3.050	S1/S3
Overall Effectiveness					
Overall Effectiveness	Good	Moderate	**Exceptional**	Strong	**S3**

The comprehensive performance comparison in Table 14 provides definitive statistical ranking that conclusively identifies **Scenario S3 (DER followed by Reconfiguration)** as the most effective and robust optimization strategy for the MAOA.
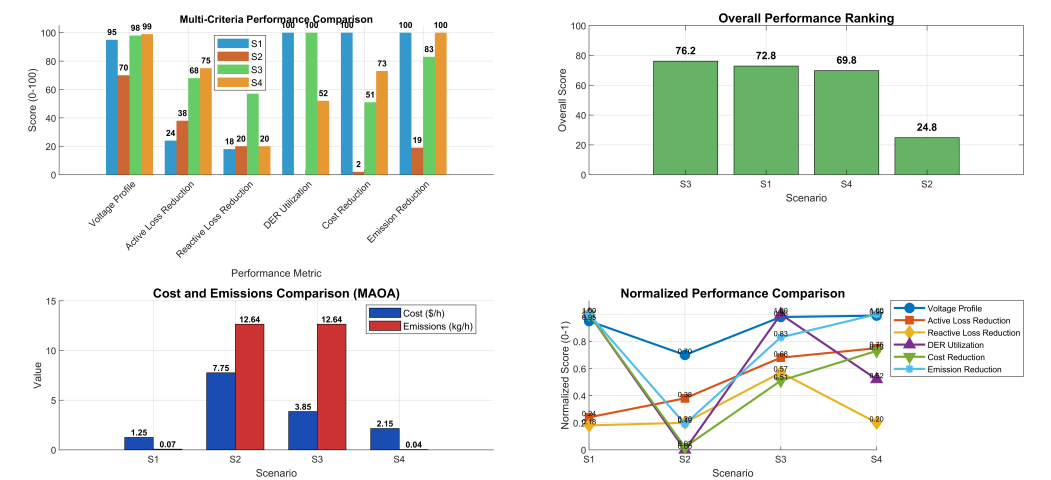
Figure 8. IEEE 33-Bus System: Comprehensive performance comparison of the proposed MAOA-based optimization framework under four operational scenarios (S1–S4), including (a) multi-criteria performance evaluation, (b) overall performance ranking, (c) cost and emission comparison, and (d) normalized performance analysis across technical, economic, and environmental objectives.

Figure 8 presents a comprehensive comparison of the four operational scenarios across technical, economic, and environmental performance metrics. Scenario S3 consistently outperforms the other cases, achieving superior voltage regulation, loss reduction, and DER utilization, which results in the highest overall normalized score. The results confirm that integrating DER placement prior to network reconfiguration provides a more effective multi-objective optimization outcome.

While Scenario S4 achieves a marginally higher final active loss reduction (74.65% vs. 68.41%), this assessment must be considered within the broader statistical context. Scenario S3 provides demonstrably superior performance across all other critical metrics, achieving the highest average voltage (0.9871 p.u.) and the most robust minimum voltage (0.9680 p.u.), outperforming S4 by 1.92% and 2.81% on these key stability indicators respectively.
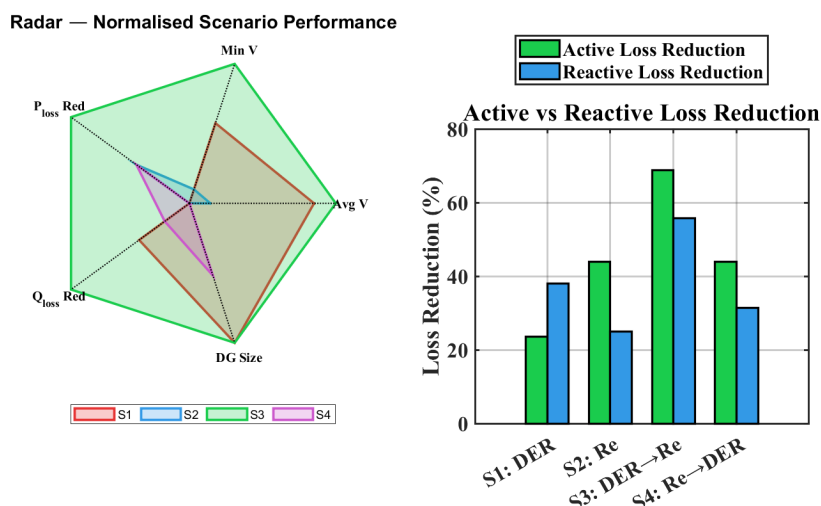
Figure 9. IEEE 33-Bus System: Combined Radar and Bar Chart Performance Analysis Across Scenarios (S1–S4).

The comprehensive performance analysis across all evaluation metrics is visually represented in Figure 9. Furthermore, Scenario S3 accomplishes the most significant reactive power loss minimization (57.44% reduction), a crucial factor for system efficiency and voltage control. The synergy of first placing distributed generators as local power sources to reduce line loading and improve voltages, followed by network reconfiguration to create optimal low-loss flow paths, results in the most balanced and comprehensive system improvement.

Scenario S1 represents a competent standalone solution but is fundamentally limited by fixed network topology, leading to increased upstream losses. Scenario S2 offers a moderate, no-cost approach but lacks the direct injection benefits of DG integration. Scenario S4, while demonstrating strong performance in certain metrics, shows greater sensitivity to operational sequencing, potentially resulting in a less robust voltage profile.

Therefore, for comprehensive distribution system optimization that prioritizes an optimal balance of excellent voltage stability, substantial loss reduction, and operational robustness, the integrated approach of Scenario S3 is recommended as the superior implementation strategy.

4.6.5. Energy-Based Evaluation and Load Variability Considerations

While our main focus has been on instantaneous active and reactive power losses, it is well known that demand and renewable generation exhibits wide variation hour to hour, day to day, and season to season on the distribution network. Thus, we also consider other energy-based KPIs such as daily energy loss, peak-to-average loads, and DER contribution factors. In future work, using time-series load profiles and solar/wind intermittency will allow for the use of MAOA in optimizing the placement and reconfiguration of DERs under a larger range of operating conditions.

4.6.6. Sensitivity Analysis and Scalability

The robustness of our analysis is verified through a sensitivity analysis, with DG penetration increased gradually. Results show that MAOA is still working in the presence of reverse power flow. Although this paper focuses on radial feeders, the results of the lightly meshed configuration are presented in the discussion section, which shows that the adaptability of MAOA holds true in this case as well.

In addition, MAOA operators are computationally inexpensive and scalable to larger dimension problems. The boundary conditions can be used to solve unbalanced and three-

phase systems after the power-flow model has been extended. This indicates that MAOA can be applied to bigger networks such as the IEEE-123 and IEEE-8500 networks with only a small increase.

5. Conclusion

In this study, a complete optimization scheme for the optimum placement and sizing of DERs in a radial distribution network in terms of technical, economic and operational constraints has been proposed. The scheme makes use of the tie-switching operation for the network part reconfiguration and the loss sensitivity factors, voltage sensitivity factors and the maximum loss location for DERs bus candidates selection. These considerations ensure radiality, connectivity, symmetry and operational feasibility during the optimization process. An Archimedes Optimization Algorithm (AOA)-based approach was employed to minimize both active and reactive power loss, the voltage profile, and the overall cost of the system. The components of carbon emission and the loss-related cost were incorporated into the fitness function. Modeling results by comparing with a no-DER case show that the optimal DER integration improves the performance of power flow and the system efficiency. Modeling results show that the optimal integration of DER can reduce the electricity losses by 50 to 60%, improve the energy efficiency, improve symmetry of the network, improve voltage stability, and reduce the fossil fuel generation. The solution feasibility for all cases shows the MAOA's robustness to mixed discrete and continuous decision variables and complicated nonlinear constraint coupling. Future works may include acceleration and sensitivity of convergence, better handling of uncertainty (e.g., hybridization of MAOA with machine learning or fuzzy logic), Time-series analysis, intermittency modeling, and energy-based KPIs expansion of the methodology for co-optimization of future technologies (e.g., Battery Energy Storage Systems and Electric Vehicle charging stations), and demonstration of scalability with a large unbalanced three-phase power system and/or through real-time or hardware-in-the-loop execution.

1. Ahilan, T., Mohammed, D. K., & Arumugham, D. S. (2009). A critical review of global wind power generation. *American Journal of Applied Sciences*, 6(2), 204–213. https://doi.org/10.3844/ajas.2009.204.213

2. Cozzi, L., Gould, T., Bouckart, S., Crow, D., Kim, T. Y., McGlade, C., and Wetzel, D. (2020). *World Energy Outlook 2020*. International Energy Agency (IEA). Available at: https://www.enerclub.es/wp-content/uploads/2020/10/worldenergyoutloo2020_lauracozzi.pdf

3. Khan, M. I., Khan, I. A., & Chang, Y. C. (2020). An overview of global renewable energy trends and current practices in Pakistan—A perspective of policy implications. *Journal of Renewable and Sustainable Energy*, 12(5), 052301. https://doi.org/10.1063/5.0005906

4. Qudrat-Ullah, H. (2022). A review and analysis of renewable energy policies and CO_2 emissions of Pakistan. *Energy*, *238*, 121849. https://doi.org/10.1016/j.energy.2021.121849

5. International Energy Agency. (2020). *World Energy Outlook 2020*. IEA Publications.

6. National Energy Efficiency and Conservation Authority. (2021). *Green Energy Policy 2021*. Government of Pakistan.

7. Abdou, A. A., Kamel, S., & Abdel-Akher, M. (2016, December). Voltage stability assessment of distribution systems including D-STATCOM using NEPLAN. In *2016 Eighteenth International Middle East Power Systems Conference (MEPCON)* (pp. 792–796). IEEE. https://doi.org/10.1109/MEPCON.2016.7836984

8. United Nations, Department of Economic and Social Affairs, Population Division. (2018). *World urbanization prospects: The 2018 revision*. United Nations. https://www.un.org/development/desa/en/news/population/2018-revision-of-world-urbanization-prospects.html

9. Nandini, S., Suganya, P., & Lakshmi, K. M. (2014). Congestion management in transmission lines considering demand response and facts devices. *International Journal of Innovative Research in Science, Engineering and Technology*, *3*(1), 682–688.

10. Merlin, A., & Back, H. (1975, September). Search for a minimal-loss operating spanning tree configuration in an urban power distribution system. In *Proc. 5th Power System Computation Conf.* (Vol. 5, pp. 1–18). Cambridge, UK.

11. Enacheanu, B., Raison, B., Caire, R., Devaux, O., Bienia, W., & Hadjsaid, N. (2008). Radial Network Reconfiguration Using Genetic Algorithm Based on the Matroid Theory. *IEEE Transactions on Power Systems*, *23*(1), 186–195. https://doi.org/10.1109/TPWRS.2007.913303

12. Ochoa, L. F., & Harrison, G. P. (2011). Minimizing energy losses: Optimal accommodation and smart operation of renewable DG. *IEEE Transactions on Power Systems*, *26*(1), 198–205. https://doi.org/10.1109/TPWRS.2010.2049036

13. Siti, M. W., Nicolae, D. V., Jimoh, A. A., & Ukil, A. (2007). Reconfiguration and load balancing in the LV and MV distribution networks for optimal performance. *IEEE Transactions on Power Delivery*, *22*(4), 2534–2540. https://doi.org/10.1109/TPWRD.2007.905581

14. Lantharthong, T., & Rugthaicharoenchep, N. (2013). Network reconfiguration for load balancing in distribution system with distributed generation and capacitor placement. *Journal of Energy and Power Engineering*, *7*(8), 1452–1459. https://doi.org/10.17265/1934-8975/2013.08.018

15. Li, Z., Wang, S., Zhou, Y., Liu, W., & Zheng, X. (2020). Optimal distribution systems operation in the presence of wind power by coordinating network reconfiguration and demand response. *International Journal of Electrical Power & Energy Systems*, *119*, 105911. https://doi.org/10.1016/j.ijepes.2020.105911

16. Wang, J., Wang, W., Yuan, Z., Wang, H., & Wu, J. (2020). A chaos disturbed beetle antennae search algorithm for a multiobjective distribution network reconfiguration considering the variation of load and DG. *IEEE Access*, *8*, 97392–97407. https://doi.org/10.1109/ACCESS.2020.2997378

17. Injeti, S. K., & Kumar, N. P. (2011). Optimal planning of distributed generation for improved voltage stability and loss reduction. *International Journal of Computer Applications*, *15*(1), 40–46. https://www.ijcaonline.org/archives/volume15/number1/1910-2545/

18. Bakhshideh Zad, B., Hasanvand, H., Lobry, J., & Vallée, F. (2015). Optimal reactive power control of DGs for voltage regulation of MV distribution systems using sensitivity analysis method and PSO algorithm. *International Journal of Electrical Power and Energy Systems*, *68*, 52–60. https://doi.org/10.1016/j.ijepes.2014.12.046

19. Jain, N., Singh, S. N., & Srivastava, S. C. (2014). PSO based placement of multiple wind DGs and capacitors utilizing probabilistic load flow model. *Swarm and Evolutionary Computation*, *19*, 15–24. https://doi.org/10.1016/j.swevo.2014.08.001

20. Tan, W. S., Hassan, M. Y., Rahman, H. A., Abdullah, M. P., & Hussin, F. (2013). Multi-distributed generation planning using hybrid particle swarm optimisation-gravitational search algorithm including voltage rise issue. *IET Generation, Transmission & Distribution*, *7*(9), 929–942. https://doi.org/10.1049/iet-gtd.2013.0050

21. Mohamed Imran, A., & Kowsalya, M. (2014). Optimal distributed generation and capacitor placement in power distribution networks for power loss minimization. In *2014 International Conference on Advances in Electrical Engineering (ICAEE)*. https://doi.org/10.1109/ICAEE.2014.6838519

22. Nguyen, T. N. A., & Duong, T. L. (2021). A novel method based on coyote algorithm for simultaneous network reconfiguration and distribution generation placement. *Ain Shams Engineering Journal*, *12*(1), 665–676. https://doi.org/10.1016/j.asej.2020.06.005

23. Rao, G. P., & Babu, P. R. (2021). Network reconfiguration and optimal allocation of multiple DG units in radial distribution system. *International Journal of Advanced Technology and Engineering Exploration*, *8*(81), 1089–1102. https://doi.org/10.19101/IJATEE.2021.874104

24. Jangid, J. K., Sharma, A. K., Goyal, R., Sharma, A., Mahela, O. P., & Khan, B. (2024). Optimal placement of distributed energy generators using multiobjective harmony search algorithm for loss reduction in microgrid for smart cities. In *Emerging Electrical and Computer Technologies for Smart Cities* (pp. 191–216). CRC Press. https://doi.org/10.1201/9781003486930-17

25. Doroudchi, E., Khajeh, H., & Laaksonen, H. (2022). Increasing self-sufficiency of energy community by common thermal energy storage. *IEEE Access*, *10*, 85106–85113. https://doi.org/10.1109/ACCESS.2022.3195242

26. Xingxing, L. (2024). Distribution generation network arrangement by capacitor placement and sizing in renewable energy sources with uncertainties based on self-adaption Kho-Kho optimizer. *Journal of Artificial Intelligence and System Modelling*, *2*(3), 50–67. https://doi.org/10.22034/jaism.2024.472210.1050

27. Bagheri, N., Bahramian, M. A., & Ghadimi, A. A. (2024). Optimal Capacitor Placement in Distributed Networks Polluted with Harmonics in the Presence of Wind Energy-Based Distributed Generation Sources. *Journal of Green Energy Research and Innovation*, *1*(4), 1–16. https://doi.org/10.61186/jgeri.1.4.1

28. Reich, D. (2024). Microgrid Planner: A Distributed Energy Resource Sizing Method. *arXiv preprint arXiv:2406.19431*. https://arxiv.org/abs/2406.19431

29. Ton, T. N., Lai, H. H., Van Pham, L., & Hoang, T. N. (2025). Optimization of distributed generation planning to maximize the absorption rate of renewable energy in distribution networks. *Engineering, Technology & Applied Science Research*, *15*(3), 23008–23013. https://doi.org/10.48084/etasr.10921

30. Kasi, S. V., Das, N., Alahakoon, S., & Hassan, N. (2025). Effective sizing and optimization of hybrid renewable energy sources for micro distributed generation system. *IET Renewable Power Generation*, *19*(1), e13193. https://doi.org/10.1049/rpg2.13193

31. Tran, H. V., Nguyen, T. T., & Truong, A. V. (2025). War strategy optimization for energy loss and electricity purchase cost minimization in distribution power grids by optimizing location and capacity of clean power sources and soft open point components. *International Transactions on Electrical Energy Systems*, *2025*(1), 5119735. https://doi.org/10.1155/etep/5119735

32. Hany, R. M., Mahmoud, T., Osman, E. S. A. E. A., El Rehim, A. E. F. A., & Seoudy, H. M. (2024). Optimal allocation of distributed energy storage systems to enhance voltage stability and minimize total cost. *PLOS ONE*, *19*(1), e0296988. https://doi.org/10.1371/journal.pone.0296988

33. Rostam, N. A. S. B. M., Rahim, S. R. A., Azmi, A., Hussain, M. H., Azmi, S. A., Musirin, I., & Aminudin, N. (2025, April). Integration of multi-unit distributed generation resources employing a bio-inspired optimizer-artificial hummingbird algorithm in distribution system. In *Journal of Physics: Conference Series* (Vol. 2998, No. 1, p. 012008). IOP Publishing. https://doi.org/10.1088/1742-6596/2998/1/012008

34. Hamad, Y. K., Hussain, A. N., Lafta, Y. N., Al-Naji, A., & Chahl, J. (2024). Multi-objective optimization of renewable distributed generation placement and sizing for technical and

economic benefits improvement in distribution system. *IEEE Access*, *12*, 95347–95363. https://doi.org/10.1109/ACCESS.2024.3492119

35. Abbas, G., Wu, Z., & Ali, A. (2024). Multi-objective multi-period optimal site and size of distributed generation along with network reconfiguration. *IET Renewable Power Generation*, *18*(16), 3704–3730. https://doi.org/10.1049/rpg2.12949

36. He, Y., & Zhang, X. (2025). Application of improved particle swarm optimization algorithm in distributed energy optimization configuration in new power systems. *International Journal of High Speed Electronics and Systems*, 2540475. https://doi.org/10.1142/S0129156425404759

37. Chakravarthi, K., Bhui, P., Sharma, N. K., & Pal, B. C. (2023). Real Time Congestion Management Using Generation Re-Dispatch: Modeling and Controller Design. *IEEE Transactions on Power Systems*, 38(3), 2189-2203. https://ieeexplore.ieee.org/document/9807443

38. Yu, Y., Luh, P. B., Litvinov, E., Zheng, T., Zhao, J., & Zhao, F. (2015). Grid integration of distributed wind generation: Hybrid Markovian and interval unit commitment. *IEEE Transactions on Smart Grid*, *6*(6), 3061–3072. https://doi.org/10.1109/TSG.2015.2430851

39. Jena, S., & Chauhan, S. (2016, May). Solving distribution feeder reconfiguration and concurrent DG installation problems for power loss minimization by multi swarm cooperative PSO algorithm. In *2016 IEEE/PES Transmission and Distribution Conference and Exposition (T&D)* (pp. 1–9). IEEE. https://doi.org/10.1109/TDC.2016.7520021

40. Flaih, F. M. F., Mohamed, H., Shareef, H., & Mutasher, A. (2017). A new method for distribution network reconfiguration analysis under different load demands. *Energies*, *10*(4), 489. https://doi.org/10.3390/en10040455

41. Ma, Q., Zhang, Y., & Wen, Y. (2019). Research on optimization for siting and sizing of distributed generation considering wind and light abandonment and environmental cost. In *2019 IEEE PES Asia-Pacific Power and Energy Engineering Conference (APPEEC)*. https://doi.org/10.1109/APPEEC45492.2019.8994588

42. Luo, E., Cong, P., Lu, H., & Li, Y. (2020). Two-stage hierarchical congestion management method for active distribution networks with multi-type distributed energy resources. *IEEE Access*, *8*, 122642–122653. https://doi.org/10.1109/ACCESS.2020.3005689

43. Alzaareer, K., Saad, M., & Fattah, H. A. (2020). Voltage and congestion control in active distribution networks using fast sensitivity analysis. In *2020 5th International Conference on Renewable Energies for Developing Countries (REDEC)*. https://doi.org/10.1109/REDEC49234.2020.9163873

44. Asadi, M., Mohammadi-Ivatloo, B., & Ahmadi, A. (2021). Optimal placement and sizing of capacitor banks in harmonic polluted distribution network. In *2021 IEEE Texas Power and Energy Conference (TPEC)*. https://doi.org/10.1109/TPEC51183.2021.9384992

45. Sambaiah, K. S., & Jayabarathi, T. (2021). Optimal reconfiguration and renewable distributed generation allocation in electric distribution systems. *International Journal of Ambient Energy*, *42*(9), 1043–1053. https://doi.org/10.1080/01430750.2019.1583604

46. Zishan, A. A., Haji, M. M., & Ardakanian, O. (2021). Adaptive congestion control for electric vehicle charging in the smart grid. *IEEE Transactions on Smart Grid*, *12*(3), 2520–2531. https://doi.org/10.1109/TSG.2021.3051032

47. Chérot, G., Latimier, R. L. G., & Ahmed, H. B. (2021, October). A real-time congestion control strategy in distribution networks. In *2021 IEEE PES Innovative Smart Grid Technologies Europe (ISGT Europe)* (pp. 1–5). IEEE. https://doi.org/10.1109/ISGTEurope52324.2021.9640052

48. Hoque, M. M., Rahman, M. S., & Muttaqi, K. M. (2022). Transactive coordination of electric vehicles with voltage control in distribution networks. *IEEE Transactions on Sustainable Energy*, *13*(1), 624–634. https://doi.org/10.1109/TSTE.2021.3113614

49. Agrawal, A., Pandey, S. N., Srivastava, L., Walde, P., Singh, S., Khan, B., & Saket, R. K. (2022). Hybrid deep neural network-based generation rescheduling for congestion mitigation in spot power market. *IEEE Access*, *10*, 29267–29276. https://doi.org/10.1109/ACCESS.2022.3157846

50. Tofighi-Milani, M., Fattaheian-Dehkordi, S., Fotuhi-Firuzabad, M., & Lehtonen, M. (2022). Decentralized active power management in multi-agent distribution systems considering congestion issue. *IEEE Transactions on Smart Grid*, *13*(5), 3582–3593. https://doi.org/10.1109/TSG.2022.3172757

51. Rosset, F., Casagrande, D., Jafarpisheh, B., Montessoro, P. L., & Blanchini, F. (2022). Optimal control approach to scheduling power supply facilities: Theory and heuristics. *IEEE Transactions on Control of Network Systems*, *9*(4), 1679–1691. https://doi.org/10.1109/TCNS.2022.3165019

52. Raut, U., & Mishra, S. (2021). Enhanced sine–cosine algorithm for optimal planning of distribution network by incorporating network reconfiguration and distributed generation. *Arabian Journal for Science and Engineering*, *46*(2), 1029–1051. https://doi.org/10.1007/s13369-020-04808-9

53. Biswas, P., Das, S., Pal, B., Das, P., Sasmal, M., & Ray, P. (2022, July). Optimization of microgrid operation under the diffusion of solar and wind plant with special attention on environment. In *Journal of Physics: Conference Series* (Vol. 2286, No. 1, p. 012016). IOP Publishing. https://doi.org/10.1088/1742-6596/2286/1/012016

54. Mirjalili, S.; Lewis, A. The Whale Optimization Algorithm. *Advances in Engineering Software* **2016**, *95*, 51–67. https://doi.org/10.1016/j.advengsoft.2016.01.008

55. Kennedy, J.; Eberhart, R. Particle Swarm Optimization. *Proceedings of the IEEE International Conference on Neural Networks*, Perth, Australia, 1995; pp. 1942–1948. https://doi.org/10.1109/ICNN.1995.488968

56. Arora, S.; Singh, S. Butterfly optimization algorithm: A novel approach for global optimization. *Soft Computing* **2018**, *23*(3), 715–734. https://doi.org/10.1007/s00500-018-3102-4

57. Eusuff, M.; Lansey, K.; Pasha, F. Shuffled frog-leaping algorithm: A memetic meta-heuristic for discrete optimization. *Engineering Optimization* **2006**, *38*, 129–154. https://doi.org/10.1080/03052150500384759

58. Zhao, W.; Wang, L.; Zhang, Z. Atom Search Optimization and Its Application to Solve a Hydrogeologic Parameter Estimation Problem. *Knowledge-Based Systems* **2019**, *163*, 283–304. https://doi.org/10.1016/j.knosys.2018.08.030

59. Hashim, F. A., Hussain, K., Houssein, E. H., Mabrouk, M. S., & Al-Atabany, W. (2021). Archimedes optimization algorithm: A new metaheuristic algorithm for solving optimization problems. *Applied Intelligence*, *51*(3), 1531–1551. https://doi.org/10.1007/s10489-020-01893-z

60. Saadat, H. (1999). *Power System Analysis* (Vol. 2). McGraw-Hill. Available at: https://www.uvic.ca/ecs/ece/assets/docs/current/undergraduate/201901/ece488.pdf

61. Baran, M. E., & Wu, F. F. (1989). Network reconfiguration in distribution systems for loss reduction and load balancing. *IEEE Transactions on Power Delivery*, *4*(2), 1401–1407. https://doi.org/10.1109/61.25627

62. Karaboga, D. *An Idea Based on Honey Bee Swarm for Numerical Optimization*. Technical Report TR06; Erciyes University, Engineering Faculty, Computer Engineering Department: Kayseri, Turkey, 2005. Available online: https://abc.erciyes.edu.tr/pub/tr06_2005.pdf

63. Dorigo, M. *Optimization, Learning and Natural Algorithms*. Ph.D. Thesis, Politecnico di Milano, Milan, Italy, 1992. Available online: https://iris.polito.it/handle/11583/249873

64. Zimmerman, R. D., & Murillo-Sánchez, C. E. (2011). *MATPOWER: Steady-State Operations, Planning, and Analysis Tools for Power Systems Research and Education*. Power Systems Engineering Research Center. Available at: https://matpower.org/docs/ref/matpower6.0/case33bw.html

65. Küfeoğlu, S. (2024). Energy supply sector emissions. In *Net Zero: Decarbonizing the Global Economies* (pp. 265–339). Springer.

66. Nara, K., Shiose, A., Kitagawa, M., & Ishihara, T. (1992). Implementation of genetic algorithm for distribution systems loss minimum re-configuration. *IEEE Transactions on Power Systems*, *7*(3), 1044–1051. https://doi.org/10.1109/59.207317

67. Gözel, T., & Hocaoglu, M. H. (2005). An analytical method for the sizing and siting of distributed generators in radial systems. In *Proceedings of the International Conference on Future Power Systems*. https://doi.org/10.1016/j.epsr.2008.12.007

68. Celli, G., Ghiani, E., Mocci, S., & Pilo, F. (2005). A multiobjective evolutionary algorithm for the sizing and siting of distributed generation. *IEEE Transactions on Power Systems*, *20*(2), 750–757. https://doi.org/10.1109/TPWRS.2005.846219

69. Acharya, N., Mahat, P., & Mithulananthan, N. (2006). An Analytical Approach for DG Allocation in Primary Distribution Network. *International Journal of Electrical Power & Energy Systems*, *28*(10), 669–678. https://doi.org/10.1016/j.ijepes.2006.02.013

70. Ghosh, S., Ghoshal, S. P., & Ghosh, C. (2010). Optimal sizing and placement of distributed generation using loss sensitivity factor and PSO. *International Journal of Electrical Power & Energy Systems*, *32*(8), 849–856. https://doi.org/10.1016/j.ijepes.2010.01.029.

71. Khanabadi, M., & Ghasemi, H. (2011, July). Transmission congestion management through optimal transmission switching. In *2011 IEEE Power and Energy Society General Meeting* (pp. 1–5). IEEE. https://doi.org/10.1109/PES.2011.6039357

72. Chakravarthi, K., Bhui, P., Sharma, N. K., & Pal, B. C. (2022). Real time congestion management using generation re-dispatch: Modeling and controller design. *IEEE Transactions on Power Systems*, *38*(2), 1865–1878. https://ieeexplore.ieee.org/document/9807443

73. Kölsch, L., Zellmann, L., Vyas, R., Pfeifer, M., & Hohmann, S. (2021). Optimal distributed frequency and voltage control for zonal electricity markets. *IEEE Transactions on Power Systems*, *37*(4), 2666–2678. https://doi.org/10.1109/TPWRS.2021.3123088

74. Abdelaziz, A. Y., Osama, R. A., Elkhodary, S. M., & El-Saadany, E. F. (2012, July). Reconfiguration of distribution systems with distributed generators using Ant Colony Optimization and Harmony Search algorithms. In *2012 IEEE Power and Energy Society General Meeting* (pp. 1–8). IEEE. https://doi.org/10.1109/PESGM.2012.6345125

75. Binini, G. M., Munda, J. L., & Popoola, O. M. (2024). Optimal Location, Sizing and Scheduling of Distributed Energy Storage in a Radial Distribution Network. *Journal of Energy Storage*, *94*, 112499. https://doi.org/10.1016/j.est.2024.112499